universität wien

MASTERARBEIT / MASTER'S THESIS

Titel der Masterarbeit / Title of the Master's Thesis

„Development of a synthetic route towards CD_2H-methyl group bearing amino acid precursors"

verfasst von / submitted by

Marilena Bisaccia BSc

angestrebter akademischer Grad / in partial fulfilment of the requirements for the degree of

Master of Science (MSc)

Wien, 2016

Studienkennzahl lt. Studienblatt / degree programme code as it appears on the student record sheet:	A 066 862
Studienrichtung lt. Studienblatt / degree programme as it appears on the student record sheet:	Masterstudium Chemie UG2002
Betreut von / Supervisor:	Univ.-Prof. Mag. Dr. Walther Schmid

ACKNOWLEDGEMENTS

I'd like to address my first words of gratitude to Professor Walther Schmid who gave me the opportunity to join his great working group and work on this thesis. Thank you for making all this possible in the first place and for always having an open door for my questions – and a variety of appropriate solution approaches at ready!

My very special thanks go to my supervisor Roman Lichtenecker, who, besides being a great scientist, is an even better teacher making him an incredibly good supervisor – actually the best I could think of. Thank you so much for your guidance, your patience and for always and without any exceptions taking time for my questions! I was never afraid of asking you a 'stupid question' because you never gave me the feeling of doing so. I also want to thank you for always finding encouraging words for me and putting everything in the right perspective!

Julia, Bettina, Gerlinde, Yuko, Christian and Manuel: you made the lab to so much more than just a working place! Thank you so much for your steady support, kindness and especially for your friendship! I will never forget about all of this!

I owe the deepest gratitude to my parents who are always there for me and who have been supporting me in every possible way. Their prudence, love, patience and confidence always guided me the right way in my life and made me the person I am today. They taught me all the real important things in life. Mama, Papa, thank you for everything! You are my role models!

I also want to thank my sisters Laura and Valeria. Lori, thank you for always being there for me with your huge heart! Thank you so much for believing in me, for your support and motivation! Leri, you always stand by me, you accompanied me through every success and every failure, making the bad times bearable and the good times real special. Thank you for being my best friend!

Last but not least, I want to express my appreciation to my fiancé for his patience, faith and support.

TABLE OF CONTENTS

1 THEORETICAL BACKGROUND

1.1 Protein NMR

Since the publication of the first Nuclear Magnetic Resonance (NMR) spectra in the journal *Physical Review* in January of 1946 by Bloch and Purcell, respectively, NMR has matured into a powerful tool regarding protein structure determination and the elucidation of dynamic processes.[1-4] While in the early stages of protein NMR the application was restricted to molecules with a size limit of 5 kDa, it is nowadays possible to analyse macromolecules up to several hundred kDa - or even 1 MDa in the case of protein complexes - via NMR spectroscopy thanks to numerous far-reaching advancements in information technology and NMR instrumentation.[1, 4-5] The most noteworthy ones among these developments are:[6]

- the application of the Fourier Transform (FT) to NMR and the conformational exploration by the Nuclear Overhauser Enhancement (NOE) in the middle of the 1960s
- the launch of the first commercially available FT NMR spectrometer by Bruker in 1969
- the introduction of two-dimensional NMR in the beginning of the 1970s
- the invention of INEPT and HMQC pulse sequences in the end of the 1970s
- the complete solvation of a protein's three-dimensional structure by NMR
- the development of three- and four-dimensional NMR for use with ^{13}C and ^{15}N labelled proteins in 1989/1990
- the introduction of TROSY, CRINEPT and CRIPT experiments for the analysis of proteins larger than 100 kDa in the late 1990s
- automated resonance assignment of proteins in 2002

Although structure determination of biological macromolecules does not represent the main focus of NMR research, today almost 10 % of all Protein Data Bank (PDB) entries are NMR-derived structures.[7] The fact that NMR spectroscopy is the only experimental method that is able to identify the structure of macromolecules as well as their dynamics and behaviour in interaction with their binding partners in native-like aqueous environment at an atomic level, distinguishes it clearly from other techniques used in structural biology.[8,9]

Proteins exhibit a notable manifoldness and complexity in their internal motion that exerts strong influence on their behaviour through a variety of mechanisms. Dynamic processes are therefore crucial for macromolecular biological functions. Of particular interest is the dynamic behaviour of methyl-bearing sidechains of hydrophobic cores, which can be well investigated by the means of ^{13}C and ^{2}H NMR relaxation studies combined with isotopic labelling strategies. NMR relaxation studies of a calmodulin complex revealed that dynamic modes might potentially be classed into categories similar to protein secondary structure motifs.[9-10] The confirmation of this finding would revolutionize the general perception of the role attributed to internal protein dynamics in molecular biological processes: the information encoded in the genome does not only determine a protein's structure but also its dynamic properties, "which means that dynamics may be an evolutionarily determined parameter of proteins" (Wand, 2001)[10]. Thus, detailed investigation of protein dynamics is substantial for a sound understanding of protein function - and NMR spectroscopy delivers the required technique for this purpose.[9-10]

Furthermore, studies of both the binding and the structure-function-relationship of proteins are of special interest for the pharmaceutical industry – a field where NMR spectroscopy is the method of choice and thus dominating other techniques like X-ray crystallography.[11]

No less relevant as the above mentioned advancements in NMR hard- and software technology has been the progresses in sample preparation. In particular, isotopic labelling methodology, which frequently triggers the design of new pulse schemes in the first place, has experienced major enhancements since the beginning of protein NMR.[12] Soon in the history of NMR spectroscopy, in the 1960s, the advantages of spectral simplification by uniform deuteration were recognized. In the 1980s random fractional deuteration was commonly used to enhance the quality of two-dimensional NMR methods. In the late 1980s uniformly ^{15}N labelled protein samples were used for three-dimensional heteronuclear methods (NOESY / TOCSY in combination with HMQC experiments). In the early 1990s, the combination of uniform ^{13}C and ^{15}N labelling and the related introduction of ^{1}H, ^{13}C, ^{15}N triple resonance experiments increased the upper size limit of proteins accessible to NMR studies to a maximum of 30 kDa.[12-15] In the 1990s one of the focal points of interest lied in experiments on highly deuterated proteins whose backbones remained protonated. This strategy made triple resonance measurements accessible to larger molecules and consequently improved backbone assignment of those molecules by the resulting decrease in relaxation times for the aliphatic ^{13}C spins and the remaining amide protons. However, at the same time the loss of the

aliphatic and aromatic protons detracts the possibility of detecting long range NOESY leading to the impairment of structural studies. The introduction of protonated methyl groups to otherwise deuterated proteins effects a compromise between a high degree of deuteration and a sufficient number of ^{1}H spins which allows structural as well as dynamic analyses.[12] A method that is perfectly suited to detect these protonated methyl groups is the TROSY experiment whose efficient application is coupled to the development of appropriate labelling strategies.[16] There exist also techniques that use special pulse schemes to suppress disturbing signals or to enhance desired ones. These approaches, however, often involve laborious instrument settings, adequate expertise and complex data-fittings. Through well-designed and robust labelling strategies a great part of this intricacy can be shifted to the sample preparation procedure.[9]

Isotopic labelling has crucially contributed to the expansion of the area of application of protein NMR and the development of new effective strategies for isotopic labelling will continue to play a substantial role in NMR research.[5]

An essential factor, which explains the fast developments in the more recent past of NMR history, is the deeper understanding of the theoretical background of the complex multinuclear, multiple-resonance and -dimensional NMR experiments. Nowadays, it is possible to predict the effect of certain pulse programs to spin systems by the profound comprehension of the density matrix equations. This allows the design of tailored pulse sequences adaptable to the respective tasks. It is this thorough understanding of the fundamental NMR physics that greatly simplified the explanation of NMR experiments and enabled access to this topic to a broader range of NMR-interested scientists.[17]

1.2 Isotope labelling

1.2.1 Aims of isotope labelling

Nowadays, most of the NMR experiments are performed with samples that are labelled with stable isotopes, whereby ^{13}C, ^{15}N and ^{2}H are used most frequently. Isotope labelling renders possible to overcome certain obstacles that otherwise encumber the analysis of larger biomolecules by NMR spectroscopy. These obstacles are mainly peak overlapping and line broadening.[18] Due to the fact that deuterium has a 6,5-fold lower gyromagnetic ratio

compared to protium, the substitution of ^{1}H by ^{2}H involves several significant advantages: on the one hand the overlap of resonance signals is reduced and on the other hand the spin-spin relaxation time is extended by diminishing dipolar relaxations mechanisms, including spin diffusion and scalar couplings. Both effects result in enhanced spectral resolution and sensitivity of homonuclear ^{1}H-^{1}H as well as of heteronuclear NMR experiments. Further improvement can be achieved by the enrichment of ^{13}C and ^{15}N.[19-21] An exiting feature of isotopic labelling is the selective incorporation of defined labelling patterns, which enables the creation of isolated spin systems opening the access to a wide field of structural and dynamic investigations.[22] An example for such an isolated spin system is the $^{13}CD_2H$-methyl group, which is the subject of this thesis.

Since the transverse dipolar relaxation rate $1/T_2^{DD}$ is directly proportional to the gyromagnetic ratio, the dipole-dipole relaxation that is induced by deuterium is 42 times weaker than that one caused by protium which affects not only the directly attached nucleus but also adjacent protons. In proteins dipolar interaction between non-carbonyl carbons and its bound protons on the one hand and the amide proton and its surrounding aliphatic protons on the other hand plays a major role in the nuclei's relaxation process. Thus, deuteration leads to an extension of the transversal relaxation time T_2 of non-carbonyl carbons and of the amide proton – in the latter case T_2 is nearly doubled. The elongated relaxation time in turn leads to reduced line widths and therefore to improved sensitivity in triple resonance experiments.[20, 23]

1.2.2 Labelling strategies

In isotopic labelling a distinction is drawn between two principal strategies: uniform and selective labelling. The experimentally less complex variant is the production of uniformly labelled proteins, which means that all atoms of a certain type are replaced by their corresponding isotopes without any selectivity. [18]

In the early history of NMR spectroscopy the above mentioned advances of incorporating deuterium into the molecule of interest have already been recognized and applied in countless NMR experiments targeting a multitude of different issues. Therefore, many different protocols for protein deuteration can be found in the literature.[13, 18] Besides the arduous chemical synthesis and semisynthesis of labelled proteins, the desired labelling patterns can also be produced in a less labour-intensive way using living cells such as bacteria or yeasts.

These organisms are capable of creating proteins from simple precursor molecules using merely aqueous solutions under mild conditions. The precise knowledge about the organism's metabolism allows not only uniform labelling but also the insertion of isotopes at specific positions.[24-25] Applying this method, the most economic and thus most frequently used technique for the production of isotopically labelled proteins is heterologous overexpression in *Escherichia Coli* (*E.coli*).[26] *E. coli* represents the most favourable host for recombinant protein expression due to its ability to rapidly produce proteins at large-scale using low-cost nutrients. Furthermore, its robustness and convenience in processing during cloning, expression and purification of the target protein makes it a valuable host. The genetics and the metabolism of *E.coli* are exceedingly well studied leading to a vast number of biotechnological tools like plasmids, fusion partners and mutant strains.[27-29]

In the case of perdeuteration (i.e. uniform deuteration) the desired protein is expressed in minimal medium containing D_2O and a deuterated carbon source.[18] Minimal media are aqueous solutions composed of the minimum nutrients needed for the growth of a bacterial culture. These minimum nutrients are limited to a carbon and a nitrogen source in addition to other salts and microelements. The carbon source can be glucose whose metabolic degradation delivers not only the carbons for the amino acid synthesis but also the energy purveyor ATP, whereas ammonium salts are in general used as nitrogen source needed for the synthesis of nitrogen-containing metabolites.[30]

The presence of deuterium causes isotope effects that reduce the efficacy of the expression process, which can - up to a certain degree - be counteracted by complying with special protocols. It is, however, the best to deliberate if total deuteration is required or not, since the deuteration rate correlates directly with the H_2O/D_2O-ratio in the culture medium. Depending on the particular task random fractional deuteration with a deuteration level of 50 % might be sufficient.[18] It should be noted that in soluble proteins the deuterons, which are incorporated at exchangeable sites (i.e. the backbone amide, the side chain amine and in some cases the thiol and hydroxide protons), usually get reprotonated during the purification steps. For some experiments, e.g. amide-detected heteronuclear 3D and 4D experiments, the reintroduction of protons is advantageous and can be improved by denaturing the target protein in an aqueous solution. However, the subsequent refolding step often proves to be rather challenging.[20, 31]

Selective deuterium labelling is achieved via the corresponding carbon source. One example for this labelling strategy is the selective incorporation of deuterated methyl groups into the

branched side chains of the amino acids valine, leucine and isoleucine using labelled α-keto acids, which will be discussed in more detail later.[32]

The most common used ammonia salts for uniform ^{15}N-labelling are chlorides, nitrates and sulphates, which are sufficient for *E.coli* bacteria to provide the nitrogen needed for the synthesis of amino acids under aerobic conditions. Since *E.coli* bacteria prefer the installation of precast amino acids rather than synthesizing them, it is possible to selectively insert labelled amino acids into the target protein. A disadvantage of this strategy is that it can only be applied to amino acids, which are endpoints of their metabolic pathway and are not further metabolized into other amino acids, which would lead to scrambling and dilution of the isotopic label. An example for isotopic scrambling is glutamate. If ^{15}N-glutamate is added as a nutrient to the medium, the resulting protein will (due to the central role of glutamate in the amino acid metabolism) not only be labelled at its glutamate sites but also to a great extent on other residues (Figure 1).[33-34] For ^{15}N-labelling there exist three possibilities to circumvent this drawback: cell-free protein synthesis, reverse labelling and the utilization of mutated *E.coli* strains.[33, 35] For example, to create an auxotroph that prevents isotopic scrambling for arginine, cysteine, glutamine, glycine, histidine, lysine, threonine, isoleucine, methionine and proline only one genetic deletion is necessary. By now, a multitude of different auxotrophic *E.coli* strains have been constructed covering a wide range of diverse labelling tasks. The Coli Genetic Stock Center (CGSC) at the Yale University represents a comprehensive *E.coli* strain database that supports the search for strains with the required properties.[34]

The reverse labelling technique is based on the same principle as the above mentioned selective labelling method with the difference that not the desired labelled amino acid is present in the growth medium but all the remaining ones in their unlabelled form along with a ^{15}N-ammonium salt. Therefore, only the missing amino acid gets newly synthesized and thus labelled.[33]

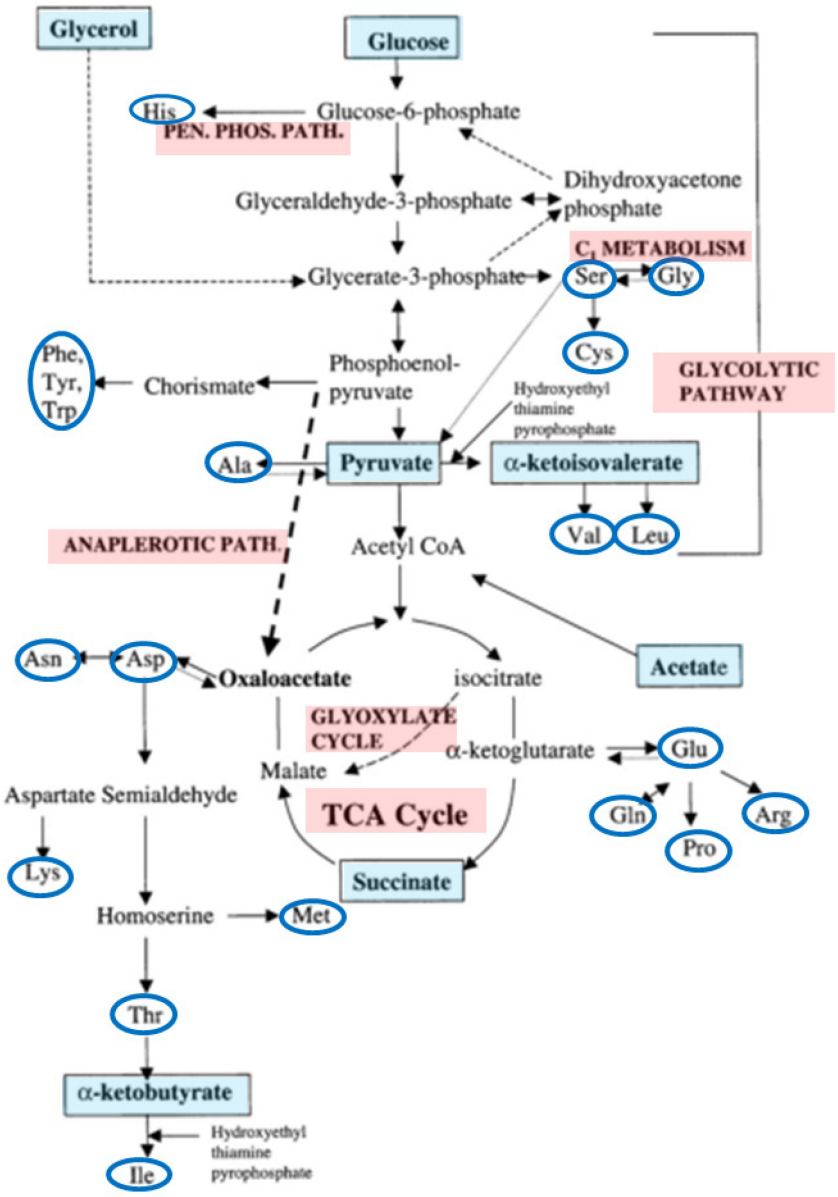

Figure 1: Schematic diagram of the amino acid metabolism in *E. coli*. The diagram shows the main metabolic pathways (highlighted in red) and the precursor molecules (boxed and highlighted in blue) that are converted into the corresponding amino acids (blue circle). As can be seen from the graphic the addition of, for example, serine, aspartate or glutamate to the growth medium leads to isotopic scrambling. The same is true for the use of precursors like succinate or pyruvate. Further it is shown that α-ketobutyrate and α-ketoisovalerate are suitable precursors for the selective labelling of isoleucine and valine/leucine, respectively. *(Adapted from: Lian et al., 2001)*

The carbon metabolism in *E.coli* for the biosynthesis of the 20 proteinogenic amino acids consists of mainly six pathways: the glycolysis, the pentose phosphate pathway, one carbon metabolism, the citric acid cycle, the glyoxylate cycle and the anaplerotic pathways. Therefore, not only ^{13}C-labelled glucose can be used as the carbon source in the growth medium but also metabolic intermediates (also referred to as amino acid precursors) like glycerol, pyruvate, α-ketoisovalerate, α-ketobutyrate, succinate and acetate (Figure 1). The decision which carbon source suits best depends on the availability and costs of the precursor, the protein yield and the desired labelling patterns. In Table 1 an overview of the generally

used and commercially available amino acid precursors and the resulting labelling patterns is provided. Glucose is directly used for the biosynthesis of amino acids through the glycolysis pathway. Therefore, the target protein is uniformly labelled with ^{13}C if [$^{13}C_6$]-glucose is added to the minimal medium as the sole carbon source.[34]

The use of [2-^{13}C]-glycerol and [1,3-^{13}C]-glycerol, respectively, along with $NaH^{13}CO_3$ as the sole carbon sources leads to alternate ^{12}C-^{13}C-^{12}C labelling of the main chain representing a possibility to expand the size limit of proteins for backbone assignments. ^{1}H-detected triple resonance experiments of uniform $^{13}C/^{15}N$-labelled proteins lose efficiency with increasing molecular size due to the fast relaxation of the ^{1}H nuclei. ^{13}C nuclei show slower relaxation due to their smaller gyromagnetic ratio compared to the ^{1}H nuclei. Therefore, ^{13}C-detected backbone assignment experiments are applicable to lager proteins and fast relaxing systems. At higher magnetic fields carbonyl carbons are unfavourable for the detection of N-C-correlations due to their high chemical shift anisotropy (CSA). Presupposed that the sample is perdeuterated, the C_α relaxation profits from the small gyromagnetic ratio in combination with a low chemical shift anisotropy. The above mentioned ^{12}C-^{13}C-^{12}C alternate labelling via [2-^{13}C]-glycerol or [1,3-^{13}C]-glycerol eliminates the scalar couplings between the C_α and the C_β or carbonyl carbon, which otherwise would decrease the nuclei's sensitivity.[36]

Alanine, leucine, isoleucine and valine share the same biosynthetic precursor, namely pyruvate. As the methyl group of pyruvate gets converted into the methyl groups of these amino acids (into the γ^2-methyl group in the case of isoleucine), pyruvate can be utilized for selective methyl group labelling (Table 1).[34]

Oxaloacetate and α-ketoglutarate, both being intermediates of the citric acid cycle, are the biosynthetic precursors of in total ten amino acids (see Figure 1). A transaminase enzyme converts oxaloacetate, α-ketoglutarate and pyruvate into aspartate, glutamate and alanine, respectively. Aspartate in turn serves as the precursor for lysine, methionine (via homocysteine), threonine and isoleucine (via α-ketobutyrate), whereas glutamate is metabolized into arginine, proline and glutamine (Table 1).[34]

Table 1: Commercially available precursors and metabolites used for uniform or selective labelling of recombinant proteins. *(Adapted from: Lian et al., 2001)*

Labelling agent	Chemical formula /structure	Incorporation sites
[$^{13}C_6$]-glucose	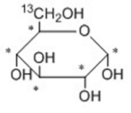	Uniform ^{13}C

[1-^{13}C]-glucose	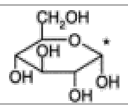	^{12}C-^{13}C-^{12}C
[$^{13}C_6$,D_7]-glucose	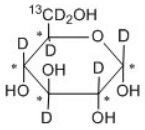	Uniform ^{13}C and perdeuteration
[D_4]-acetate	CD_3CO_2D	Perdeuteration
[$^{13}C_2$]-Acetate	$^{13}CH^{13}CO_2H$	Uniform ^{13}C
[4,4′-^{13}C]-α-ketoisovalerate	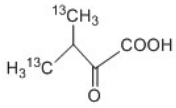 in H_2O	(^{13}C-δ-methyl)-leucine; (^{13}C-γ-methyl)-valine
[3-D]-^{13}C-α-ketoisovalerate	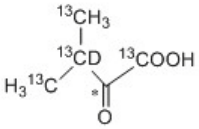 in D_2O	($^{13}C^1$H-δ-methyl)-leucine and ($^{13}C^1$H-γ-methyl)-valine selective methyl protonation
[4-^{13}C]-α-ketobutyrate	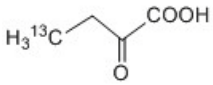 in H_2O	(^{13}C-δ1-methyl)-isoleucine
[3,3′-D_2]-^{13}C-α-ketobutyrate	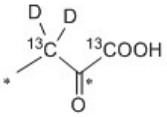 in D_2O	($^{13}C^1$H-δ_1-methyl)-isoleucine selective methyl protonation
[2-^{13}C]-glycerol	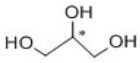	^{12}C–^{13}C–^{12}C
[1,3-$^{13}C_2$]-glycerol	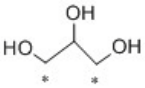	^{12}C–^{13}C–^{12}C
[D_8]-glycerol	(OD)-CD_2-CD-(OD)-CD_2-(OD)	Perdeuteration
[$^{13}C_3$]-pyruvate	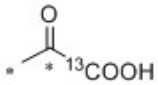 in D_2O	(^{1}H-δ-methyl)-leucine, (^{1}H-γ-methyl)-valine, (^{1}H-γ2-methyl)-isoleucine, (^{1}H-β-methyl)-alanine uniform ^{13}C-labelling
[3-^{13}C]-pyruvate	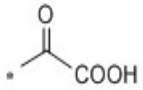 in H_2O or D_2O	(^{13}C-δ-methyl)-leucine; (^{13}C-γ-methyl)-valine; (^{13}C-γ2-methyl)-isoleucine; (^{13}C-β-methyl)-alanine
[D_6]-succinate	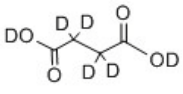	Perdeuteration

α-Ketobutyrate is a precursor of isoleucine and can thus be utilized for isoleucine selective labelling and the integration of certain labelling patterns like the insertion of a $^{13}CH_3$ methyl group in an otherwise ^{12}C and deuterium containing residue.[34] The direct precursor of isoleucine is α-keto-β-methylvalerate, which is transformed to isoleucine by the enzymes

leucine dehydrogenase and branched-chain amino acid aminotransferase.[37-38] α-Keto-β-methylvalerate has already been successfully applied as a precursor for isoleucine labelling.[39]

The use of isotopic labelled α-ketoisovalerate as the sole carbon source in the growth medium leads inseparably to the simultaneous labelling of leucine and valine. A possibility to separately label these two amino acids was found downstream (from α-ketoisovalerate) in their biosynthetic pathway. Valine is directly formed from α-ketoisovalerate, whereas in the case of leucine α-ketoisovalerate is first converted into α-ketoisocaproate. Hence, the independent selective labelling of valine and leucine can be controlled by the addition of either labelled α-ketoisocaproate (for selective leucine labelling) or unlabelled α-ketoisocaproate in combination with labelled α-ketoisovalerate (for selective valine labelling) to the growth medium (Figure 2). Figure 3 shows the comparison between two ^{13}C-HSQC spectra of his-tagged GB1, a 7,5 kDa model peptide. Spectrum A was taken from the model peptide, which was overexpressed in minimal medium containing sodium-($^{13}CH_3$)-2-ketoisovalerate and glucose as the sole carbon sources. As a result both amino acid residues, leucine and valine, were ^{13}C-labelled. If the overexpression medium is in contrast supplemented with (unlabelled) sodium-2-ketoisocaproate in the same concentration as sodium-($^{13}CH_3$)-2-ketoisovalerate, only valine gets labelled, which can be seen in spectrum B.[40-41]

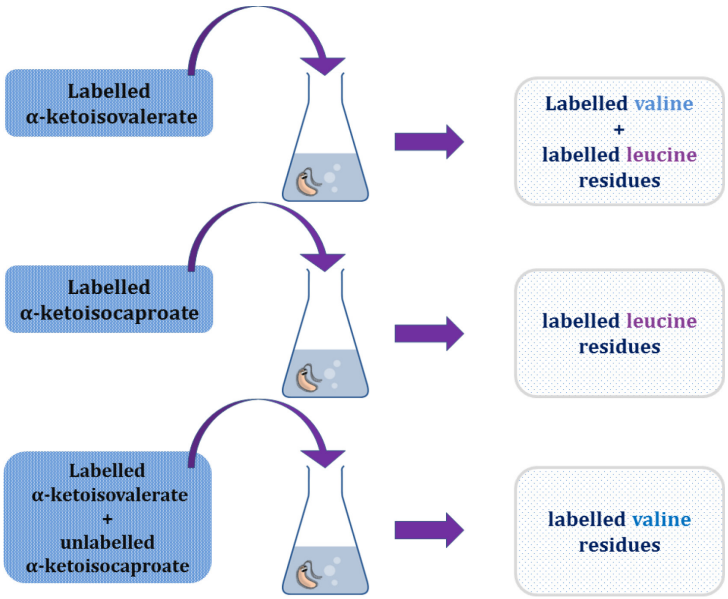

Figure 2: Schematic draw of the labelling strategy for independent valine and leucine ^{13}C-labelling. The blue boxes on the left side indicate which precursor(s) must be added to the $^{15}NH_4Cl$ and glucose containing minimal medium to obtain labelled valine and leucine/ only labelled leucine/ only labelled valine residues (white boxes on the right). The Erlenmeyer flasks stand for the *E.coli* overexpression process. *(Adapted from: Lichtencker et al., 2013)*

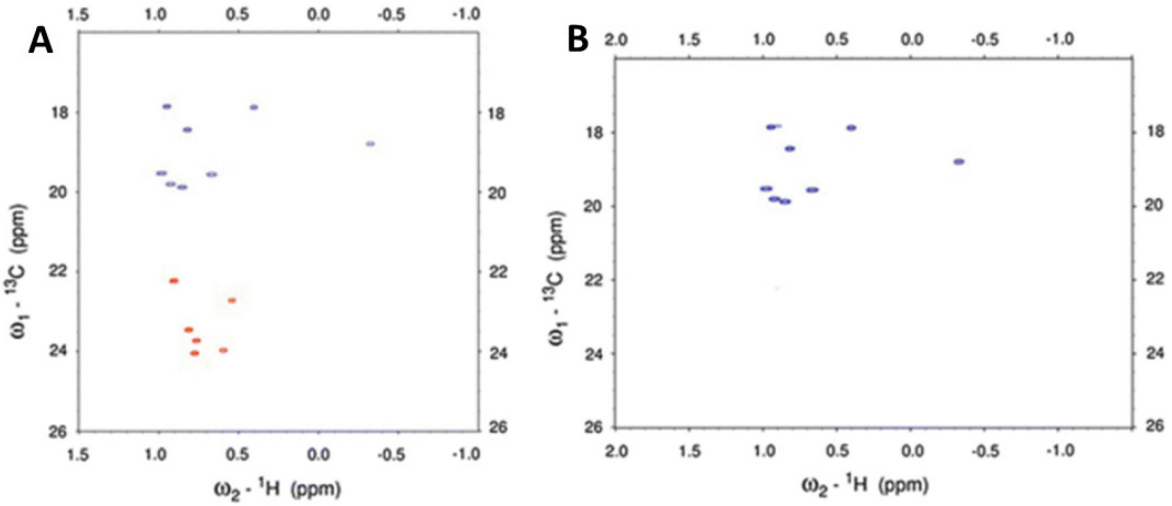

Figure 3: ^{13}C-HSQC spectra of his-tag-GB1. In spectrum A his-tag-GB1 was expressed in presence of sodium-($^{13}CH_3$)-2-ketoisovalerate. Therefore signals form valine as well as from leucine are visible. Spectrum B lacks the leucine signals because the target peptide was expressed in presence of sodium-($^{13}CH_3$)-2-ketoisovalerate and sodium-2-ketoisocaproate. *(Adapted from: Lichtenecker et al., 2013)*

1.3 The use of methyl groups in NMR experiments

As discussed above, solution NMR spectroscopy represents an indispensable tool in elucidating protein function and mechanism thanks to its unique capability of investigating the dynamics of macromolecules at an atomic level and under native-like conditions.[42] Methyl groups bearing amino acid residues are particularly valuable NMR probes for this purpose since they are enriched at protein interacting surfaces and in hydrophobic cores. Up to 24 % of the protein-protein interface amino acids possess methyl groups; in hydrophobic cores this share may rise up to 50 %.[4] For this reason, NOEs between methyl group protons deliver beneficial structural restraints.[12] Besides their favourable position within critical core regions of folded proteins, methyl groups offer advantageous relaxation behaviour. [43-44] Their relaxation process is – equally to the relaxation of the whole protein - mainly dominated by dipole-dipole coupling (DD) between the spin-1/2 particles ^{13}C and ^{1}H and the chemical shift anisotropy of each single spin. Both, DD and CSA are in turn modulated by rotational

molecular motions. The interference of these two relaxations types can be exploited via attuned pulse schemes to suppress transverse relaxation and thus enhance the spectral sensitivity and resolution. [45]

Methyl groups relax through a vast network of cross-correlated interactions that interconnect the 10 ^{1}H and 8 ^{13}C intra-methyl single quantum transitions as well as the methyl group itself with surrounding spins. The latter interaction considerably affects the relaxation properties of the methyl group protons. [17, 46] The very fast rotation of the methyl group about its threefold axis against the background of the slow overall molecular motion causes interference between intra-methyl dipolar correlations. This interference in turn leads to certain ^{1}H-^{13}C multi and ^{1}H-^{1}H single quantum transitions of which relaxation is not affected by intra-methyl dipolar fields. This results in the cancellation of certain relaxation pathways leading to partly decreased relaxation rates and thus to a net reduction of transverse relaxation. Since transverse relaxation is a major obstacle regarding the size limit of macromolecules to be analysed, the constructive interference of dipole-dipole coupling and chemical shift anisotropy expands the limits of protein NMR. This phenomenon is referred to as the TROSY effect as it represents the basis of transverse relaxation optimized spectroscopy (TROSY). [12, 45-46] In HMQC experiments, which are well suited for TROSY correlation spectroscopy because of the applied pulse programs, 50 % of the initial ^{1}H and ^{13}C magnetisation is decomposed via fast relaxation pathways, whereas the other half exhibits far longer relaxation times. If the interaction of neighboured non-methyl protons is prevented, there will be no interchange between the slow and fast relaxing pathways. This means that the favourable slow relaxing pathways stay unaffected by the fast relaxing mechanisms and can be analysed separately. The possibility of filtering out TROSY effect conducted pathways gives this sort of experiment a substantial edge compared to methods that do not exploit the TROSY effect like HSQC schemes. In HSQC approaches fast and slow relaxing components get interconverted which has as a consequence a decline in sensitivity and resolution.

The interaction of the methyl group with neighboured protons has an adverse impact on the methyl TROSY effect. For this reason TROSY based measurements are performed by inserting protonated methyl groups into perdeuterated proteins. This technique is therefore another example for the fundamental importance of labelling strategies and their constant further development.[16]

Two further applications represent the measurement of dynamic processes at millisecond scale and the determination of side chain order parameters via the measurement of intra-methyl ^{1}H-^{13}C/^{1}H-^{1}H cross-correlation rates or via relaxation analysis of the deuterium spin.[47]

Although methyl-TROSY experiments made a profound contribution to expand the size limit of proteins that are accessible to NMR investigation, the positive influence of the TROSY-effect still diminishes with increasing size of the target protein. The higher the molecular weight the more difficult it becomes to obtain good resolutions. One attempt to tackle this problem represents the development of HZQC (heteronuclear zero quantum coherence), a zero quantum analogue of the HMQC scheme. In HZQC experiments special pulse sequences are used to minimize the dipolar interaction between the methyl group spins and the spins of the surrounding deuterons and neighboured methyl protons in methyl protonated, perdeuterated proteins. This procedure leads, besides line narrowing of the signals, also to a slight loss in sensitivity compared to HMQC data (around 10 %). The distinct gain in resolution, however, compensates this loss by far so that HZQC experiments can be considered as a valuable tool for large proteins [48]

1.3.1 The application of deuterated methyl groups

After methyl groups had turned out to be excellent probes for structural and dynamic studies on large proteins it was considered whether the substitution of protons by deuterons could offer additional advantages. It is obvious that the replacement of protons by deuterons affect the magnetisation and the relaxation properties of the whole methyl group. The lower number of ^{1}H spins that may contribute to transverse relaxation mechanisms might increase the transverse relaxation time but at the same time it might lead to the undesired extension of the longitudinal relaxation time since less protons provide the NMR signal with their steady-state polarization.[47]

The three methyl isotopologues CH_3, CH_2D and CHD_2 differ in their respective relaxation behaviour due to the different number of protons.[47] The CHD_2 methyl isotopologue owns a spin system that can be compared with an AX-like type of spin system which means a simplification of the prevailing relaxation mechanism.[49] Ollerenshaw et al.[47] have developed pulse schemes optimized (in regard of signal to noise ratio and resolution) for each

isotopologue in order to be able to properly compare their suitability as probes in structural studies of proteins. For the $^{13}CH_3$ methyl group an adapted version of the above mentioned $^{13}CH_3$ HZQC pulse sequence was employed. CH_2D and CHD_2 methyl groups were detected by newly developed pulse schemes called CH_2D TROSY and CHD_2 HZQC, respectively. The resulting spectra are shown in Figure 4. It was found that the CH_3 methyl isotopologue recorded with HMQC or $^{13}CH_3$ HZQC pulse sequences fits best as a probe in structural studies of proteins. The reasons are on the one hand the greater sensitivity due to the higher number of ^1H spins and on the other hand the fact that CH_3 methyl groups possess a shorter longitudinal relaxation time. Moreover, in $^{13}CH_3$ HMQC measurements the separation of fast and slowly relaxing mechanisms occurs automatically, whereas in the other two pulse schemes additional pulse elements have to be applied which are responsible for a great part of the sensitivity loss. The gain in sensitivity of a $^{13}CH_3$ HMQC spectrum compared to a CHD_2 HZQC spectrum is of a factor of 2,4. [47]

For studies that have other targets than structural analyses $^{13}CH_2D$ and $^{13}CHD_2$ methyl groups render valuable facilitation. These other targets include the investigation of side chain dynamics via ^2H spin relaxation determination or the detailed analyses of relaxation in methyl spin systems via the comparison of the different isotopologues.[47]

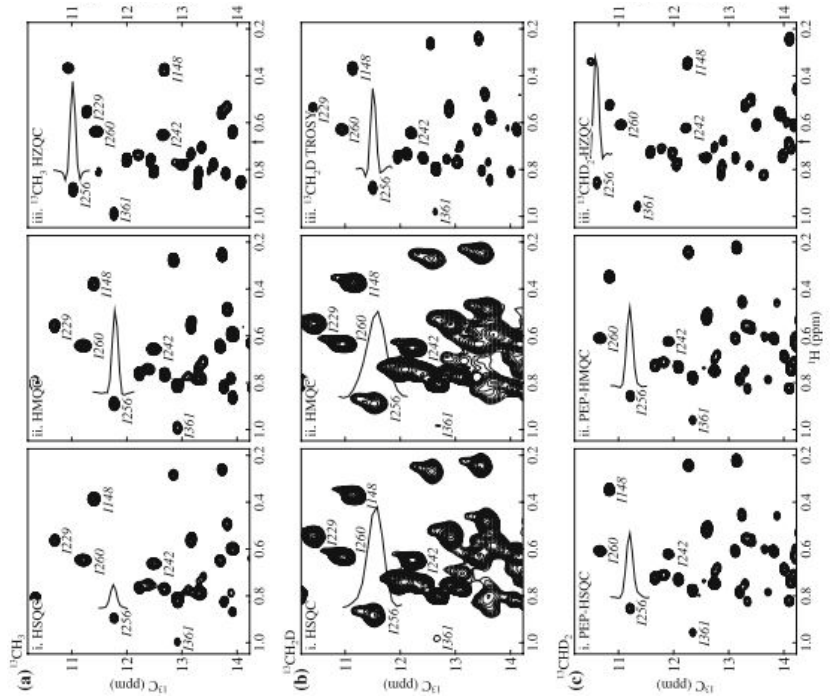

Figure 4: Comparison of HSQC (i), HMQC (ii) and the respective optimized pulse sequence (iii) spectra of $^{13}CH_3$, $^{13}CH_2D$ and $^{13}CHD_2$ methyl groups in MSG. All spectra are normalized to the same noise background and plotted at the same contour level. The peak intensities are hence directly comparable. For better comparison a few assignments to isoleucine δ1 methyl groups are delineated and a trace along the indirectly detected dimension through the peak corresponding to isoleucine 256 is shown in each spectrum. *(Reproduced from: Ollerenshaw et al., 2005)*

1.3.2 $^{13}CH_2D$ /$^{13}CHD_2$ methyl groups as probes for the study of dynamic processes

The shift between a protein's active and inactive form is in many cases indicated by conformational changes in the microsecond to millisecond time scale. These relatively slow motions are believed (and in many cases already proven) to be rate limiting in essential biological processes like protein folding, substrate/ligand binding, enzymatic catalysis, allosteric regulation, product release and target recognition. Thus, the analysis of these conformational fluctuations gives precious insight into dynamic processes. While protein backbone atoms have been the subject of many studies, investigations of the side chains prove to be more challenging and were at first restricted to shorter time scales. For that purpose isolated $^{13}CHD_2$ probes (isolated means that the methyl group is mainly surrounded by ^{12}C and ^{2}H) have successfully been introduced as they are for several reasons optimal reporters for the investigation of chemical exchange via relaxation dispersion experiments.[50-51] These reasons include the fact that the major part of the methyl ^{13}C transverse relaxation runs over the single attached proton; the contribution of the two deuterons together account for just 12 % of the transverse relaxation rate R_2. Therefore, the ^{13}C nucleus of the $^{13}CHD_2$ group has a relatively small R_2 value. The two other expedient reasons are the absence of ^{1}H-^{13}C cross-correlation relaxation and direct ^{13}C-^{13}C scalar and dipolar couplings. [51]

A possibility to perform relaxation dispersion measurements is the Carr-Purcell-Meiboom-Gill method that determines the relaxation rate R_2 by plotting the signal decay as a function of time. [52-53] This method originates from the year 1950 when Hahn published his paper about spin echoes and was further developed by Carr and Purcell in 1954 and by Meiboom and Gill in 1958.[54-56] The method presented by Hahn uses repetitive 90° and 180° pulse sets that are separated by a time interval required to restore the system's thermal equilibrium condition. The time dependence of the signal decay is detected by varying the time constant τ which stands for the time between the 90° and 180 ° pulse. Carr and Purcell concluded that the application of only one single 90° pulse followed by several 180° pulses with τ being smaller than the natural lifetime of the nuclear signal was a possibility to largely eliminate the 'artificial' decay caused by diffusion. In fact, the relaxation rates calculated on the basis of these two methods deliver the same results for viscous solutions where diffusion plays a minor role. In non-viscous samples, however, diffusion contributes strongly to the relaxation process and thus the relaxation rate determined on the basis of Hahn's method differs clearly from the one calculated with the method modulated by Carr and Purcell.[55] Though the application of successive 180° pulses reduces the error caused by diffusion, it creates a new

problem: if the 180° pulses deviate from the correct amplitude value, these deviations accumulate with every further pulse and rotate the polarisation vectors successively out of the detection plane leading to severe errors in the results. Meiboom and Gill solved this issue by introducing the two following modifications: first they applied phase coherent 180° pulses, which means that, from the rotating frame of reference, the direction of the radio frequency field is the same for all pulses. Secondly, they shifted the direction of the radio frequency field of the 90° pulse by 90° relative to the 180° pulses. The consequence of these two modifications is that all echoes have the same phase so that amplitude deviations of the 180° pulses are automatically compensated at every second pulse. [56]

In summary, the $^{13}CH_2D$ but especially the $^{13}CHD_2$ methyl group is an excellent probe for the investigation of dynamic processes of proteins and the Carr-Purcell-Meiboom-Gill method is well suited for this purpose as it offers access to the required data. Thus, the design of strategies for the selective incorporation of deuterated methyl groups represents an important field of research.

1.3.3 Synthesis of $^{13}CH_2D$ and $^{13}CHD_2$ methyl groups

So far, there are two major strategies that are used to obtain access to $^{13}CH_2D$ and/or $^{13}CHD_2$ methyl groups.

The first strategy focuses on the development of pulse schemes that allow the selective detection of these methyl groups from a mixture of $^{13}CH_3/^{13}CH_2D/^{13}CHD_2$ methyl isotopologues. The isotopologue mixture can be obtained by expressing the protein sample in a minimal medium containing D_2O as solvent and protonated ^{13}C-labelled pyruvate as the carbon source. The challenge in this approach is to suppress the signal of the $^{13}CH_3$ methyl group, which delivers the strongest peak among the different isotopologues without provoking too severe sensitivity losses for the other two isotopologues. To this end purging elements that cause dephasing of the magnetisation terms of ^{1}H-spin including $^{13}CH_3$ spins systems are introduced into the pulse schemes. Unfortunately, this concept loses its efficiency with increasing molecular weight of the sample. An option to completely exclude $^{13}CH_3$ signals is to transfer magnetization through deuterium but the accompanying loss of more than 50 % of the signal intensity of $^{13}CHD_2$ methyl groups restricts this technique to experiments seeking for deuterium relaxation analysis.[49] A more generally applicable method is to use partially deuterated pyruvate-3-^{13}C (50-60 % deuterium at position 3) to reduce the amount of CH_3 isotopologues. If additional partially deuterated sodium 4-^{13}C –ketobutyrate is included into the expression culture besides the partially deuterated pyruvate, an increased rate of $^{13}CH_2D$

and $^{13}CHD_2$ labelled methyl groups in isoleucine residues (position δ and γ^2) is achieved. Ishima and co-workers attained a clear reduction of the CH_3 level by the use of 4-^{13}C,3,3,4,4,4-D_5 2-ketobutyrate (98 % 3-D_2; 62 % 4-D_3; 99% 4-^{13}C) and 3-^{13}C,3,3,3-D_3 pyruvate (50-60 % 3-D_3; 99 % 3-^{13}C). The intensity ratios of CH_3 to CHD_2 of leucine, valine, isoleucine ($C^{\gamma 2}$) and isoleucine (C^{δ}) residues were 3.2 %, 2.7 %, 3.8 % and 7.6 %, respectively.[57]

The second strategy is to add commercially available α-keto acid precursors to the culture media that already carry the desired isotopologue. For selective labelling of isoleucine methyl groups (C^{δ}) α-ketobutyrates is used, whereas for valine and leucine residues α-ketoisovalerate is applied. The possibility of selectively introducing methyl groups with the desired labelling pattern into the target protein in combination with sophisticated pulse schemes clearly widens the access to lager protein samples and therefore represents an important contribution to protein NMR.[58-61] Although the convenience of readily purchasable precursors is an obvious advantage, this convenience comes with high costs (Table 2). Thus, it is of great interest to design a cost-effective and robust synthetic route for the production of $^{13}CH_2D$ and $^{13}CHD_2$ labelled α-keto acid precursors, which was the aim of this master's thesis.

Table 2: Commercially available α-keto acid precursors.

Substance	Structure	Commercial source / price (pack size)
Sodium α-ketoisovalerate-3-(methyl-^{13}C,D_2),4-^{13}C,D_2	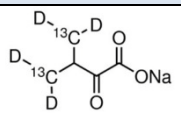	Sigma Aldrich 1640 € (250 mg)[a, d]
Sodium α-ketobutyrate-4-^{13}C, D_2	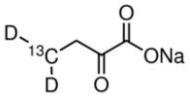	Sigma Aldrich 2725 € (500 mg)[a, d]
Sodium α-ketobutyrate-4-^{13}C,D	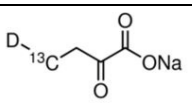	Sigma Aldrich 660 € (100 mg)[a, d]
Sodium α-ketoisovalerate-3-D,(methyl-D_3),4-^{13}C,D	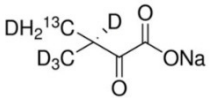	Sigma Aldrich Price upon request [a]
Sodium α-ketoisovalerate-3-D,(methyl-D_3),4-^{13}C,D_2	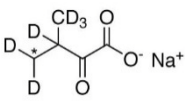	Euriso-Top 1106 € (250 mg)[b]
Sodium α-ketobutyrate-3-D_2, 4-^{13}C, D_2	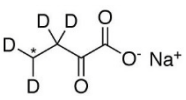	Euriso-Top 1250 $ (250 mg)[c, e]

a: http://www.sigmaaldrich.com/chemistry/stable-isotopes-isotec/stable-isotope-products.html?TablePage=12514389

b: http://www.eurisotop.com/search?searchValue=cdlm-7354

c: http://shop.isotope.com/productdetails.aspx?id=10032298&itemno=CDLM-7353-PK

d: Protons at C-3 can be quantitatively exchanged to deuterium according to Goto et al. or Gardner et al.[62-63]

e: Listed price applies for orders within North America. Additional shipping fees occur for orders outside of North America.

1.4 The Wittig Reaction

As the Wittig Reaction represents the key and at the same time the most challenging reaction step in the synthetic route presented in this master's thesis for the production of $^{13}CHD_2$ labelled α-keto acid precursors, it is discussed in more detail in the following section.

Already in 1919, during the course of their search for new phosphorus compounds, Staudinger and Meyer figured out that the reaction of phenylisocyanate with the phosphine methylene derivative $(C_6H_5)_3P{=}C(C_6H_5)_2$ results in the olefination of the carbonyl function of phenylisocyanate.[64-65] But since Staudinger and Meyer attached more importance to the yielded imine product than to the remarkable reaction *per se*, another 34 years passed until Georg Wittig published his work on the reactions of pentaphenyl phosphorus and its derivatives describing his observation that in the reaction of methylenetriphenylphosphorane with benzophenone the carbonyl group of benzophenone is replaced by the methylene group of methylenetriphenylphosphorane.[65-67] This reaction, which was later on referred to as the Wittig Reaction, is not restricted to benzophenone as a reactant and can generally be used for the regiospecific olefination of carbonyl functions. The essential usefulness of this versatile reaction for preparative organic chemistry was soon recognized and found rapidly entrance into industrial processes like for example the production of vitamin A and β-carotene. Nowadays, the Wittig Reaction is one of the most commonly used methods for the preparation of alkenes. Wittig's important work was honoured by the awarding of the Nobel Prize in Chemistry in 1979.[66, 68]

1.4.1 Reaction scheme, reactants and reaction conditions

The Wittig Reaction refers to the reaction between a carbonyl compound (aldehyde or ketone in general) and a phosphonium ylide to the corresponding alkene and phosphine oxide (Figure 5). The structure of the phosphonium reagent can be written as the ionic ylide form or as the ylene form. These two forms should not be understood as resonance structures but should underline the ionic character of the bond between the carbon and the phosphorus. [68-69]

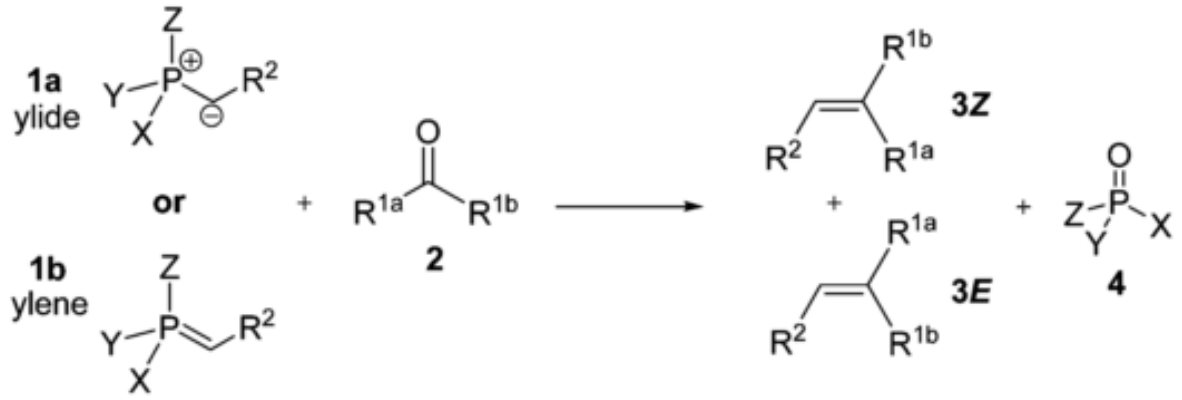

Figure 5: The Wittig Reaction. X, Y and Z may each be an alkyl, aryl or alkoxy group. R^2 may be an alkyl, aryl, vinyl, or an electron withdrawing group. The carbonyl compound (2) may an aldehyde or a ketone. *(Reproduced from: Byrne/Gilheany, 2013)*

The desired ylide is generated by the addition of a base to the corresponding phosphonium salt.[69] Depending on the attached substituents, three different types of ylides are distinguished: stabilised, semi-stabilised and non-stabilised ylides. Non-stabilised or reactive ylides carry an alkyl group as a substituent and are hydrolytically labile. If the substituent is a phenyl or alkenyl group, the ylide is classified as semi-stabilised and less susceptible to hydrolysis. Stabilised ylides refer to ylides of which C_α substituent is an electron-withdrawing group such as an ester or a cyano group. If the ylide is in addition derived from a triphenylphosphine salt, the resulting species – unlike the former two ylide types – is stable against ambient moisture. An interesting feature of the Wittig Reaction is that the stereoselectivity is determined by the ylide's character (Figure 6). This holds particularly true for triphenylphosphine ylides where the extent of anion stabilisation dictates whether the formation of the *E*- or the *Z*-isomer is preferred.[68]

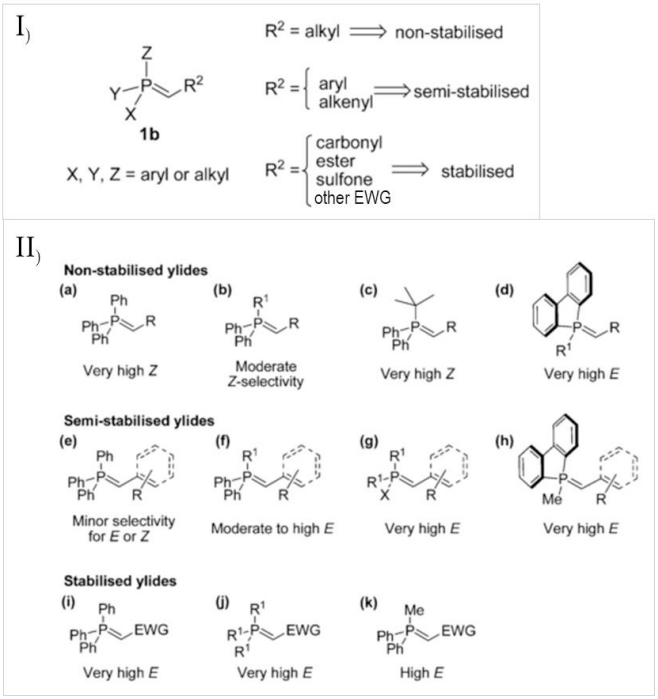

Figure 6: Ylide classification. I): The degree of stabilisation is determined by the substituent R^2 (EWG= electron-withdrawing group). II): The nature of the ylide influences the stereoselectivity for the *E/Z*-isomers. *(Adapted from: Byrne/Gilheany, 2013)*

The reaction conditions of the Wittig Reaction are usually mild requiring relatively low temperatures and common solvents, e.g. THF, DMF, chloroform, alcohols etc. [68, 70]

For the preparation of non-stabilised ylides inert conditions and relatively strong bases are required like *n*-butyllithium, whereas for stabilised ylides weaker bases such as alkali hydroxides are sufficient.[69]

1.4.2 Reaction mechanism

The elucidation of the mechanism of the Wittig Reaction has been – and partially still is – the subject of numerous studies. A distinction between two principal types of the Wittig Reaction should be drawn: the lithium present and the lithium salt-free mechanism. While the latter mechanism is deemed to be solved, the lithium present one is still unknown. [68]

The most contentious issue regarding the mechanism is which and how many intermediates are formed during the reaction. Wittig originally assumed that only one single intermediate species is involved and suggested that species to be a betaine. It was soon recognized that a second species is involved, namely oxaphosphetane. The proposed mechanism, which includes both intermediates, describes the formation of the betaine via nucleophilic addition of the ylide to the carbonyl compound and subsequent ring closure giving the

oxaphosphetane. The oxaphosphetane is then decomposed to an alkene and phosphine oxide (Figure 10). Since the betaine has been attributed a more important role than the oxaphosphetane, this mechanism is referred to as the betaine mechanism [68-69]

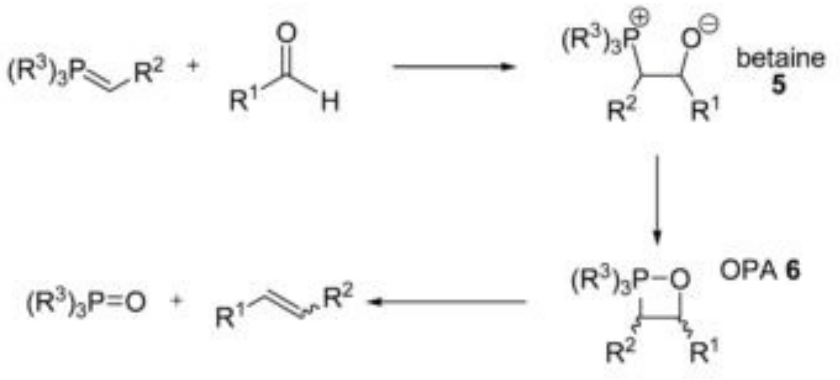

Figure 7: The betaine mechanism of the Wittig Reaction. The ylide nucleophilically attacks the carbonyl group to build the betaine. Via a ring closure reaction the oxaphosphetane is formed. The decomposition of the oxaphosphetane delivers the alkene and phosphine oxide. (*Reproduced from: Byrne/Gilheany, 2013)*

In the last few decades numerous different mechanisms have been brought forward like the Bergelson's 'C–P–O–C' betaine mechanism, the Schweizer mechanism, Olah's single electron transfer mechanism, Bestmann's 'P–O–C–C' betaine mechanism or the Schlosser cycloaddition mechanism, to name just a few.[68] All of these proposed mechanisms have a common denominator, they cannot account for the experimental evidences that are now available thanks to computational and low temperature NMR studies.[68-69] A mechanism that complies with the current evidences provides the formation of the oxaphosphetane via an irreversible [2+2] cycloaddition as the first step, where the stereochemistry of the alkene is determined during the formation of the oxaphosphetane. It is believed that the decomposition of the oxaphosphetane happens in a single step that includes a Berry pseudorotation and a P-C/C-O bond breakage (Figure 8).[68]

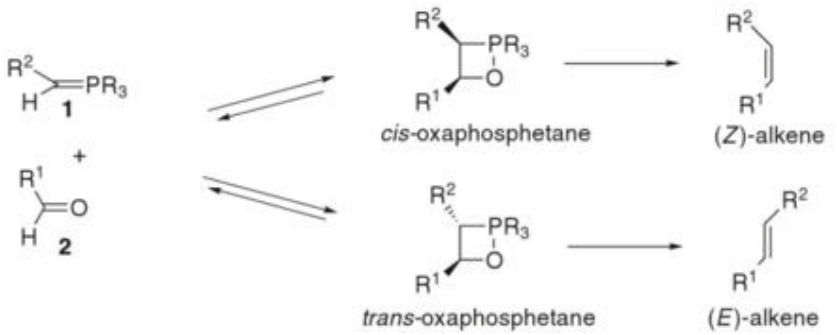

Figure 8: The mechanism of the lithium salt-free Wittig Reaction. The oxaphosphetane is formed via an irreversible [2+2] cycloaddition and decomposed in a single step to give the product alkene. (*Reproduced from: Edmonds/Abell, 2004)*

2 OBJECTIVE AND BASIC CONCEPT OF THE MASTER'S THESIS

The aim of this master's thesis was the development of new synthetic routes for the production of a leucine and an isoleucine precursor that are both labelled with a $^{13}CHD_2$ methyl group. Beside the introduction of this special labelling pattern, the use of inexpensive educts was strived. This was achieved by the use of D_2O as the deuterium source and ^{13}C-iodomethane as the ^{13}C source. The fundamental importance of selectively labelled amino acid precursors for NMR based research of proteins is described in detail in the preceding chapter. The fact that several of such precursors are commercially available does not undermine the intention of this thesis, since they are hitherto exceedingly expensive.

The leucine precursor α-ketoisocaproate was opted as it allows the selective labelling of leucine (see chapter 1.2.2). For isoleucine α-keto-β-methylvalerate was chosen (see chapter 1.2.2). The basic concept was to start with a compound, which can be transformed into α-ketoisocaproate or α-keto-β-methylvalerate within a few reaction steps and which carries a carbonyl group at a certain position. This carbonyl group is used to introduce deuterium and ^{13}C via the Wittig Reaction with deuterium- and ^{13}C-labelled methyltriphenylphosphonium iodide (Wittig Salt). The oxygen of the carbonyl group is thus replaced by a CD_2 group. The methylene group is subsequently reduced by hydrogen gas in the presence of a palladium on carbon catalyst to give a CHD_2 methyl group. The following deprotection yields α-ketoisocaproate/ isobutyraldehyde or α-keto-β-methylvalerate. In the case of isobutyraldehyde the next reaction step is an aldol condensation with hydantoin. The obtained 5-isobutylidene hydantoin is subsequently reacted with NaOH to yield sodium α-ketoisocaproate.

The following six compounds were chosen as educts for the Wittig Reaction:

Table 3: Reactants used for the Wittig Reaction.

Leucine precursors	
Ethyl 4-oxo-2,2-(propylenedioxo)-pentanoate (1)	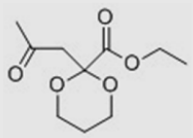
Methyl 2,2-dimethoxy-4-oxopentanoate (2)	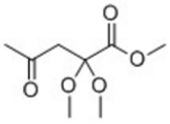
3-((tert-butyldimethylsilyl)oxo)-2-propanone (4)	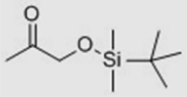
1-(tetrahydropyran-2-yloxy)-2-prpanone (6)	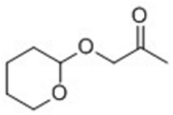
Isoleucine precursor	
Methyl 2,2-dimethoxy-4-oxobutanoate (5)	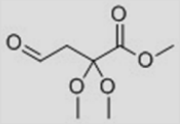
testing compound	
4,4-Dimethoxy-2-butanone (3)	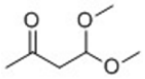

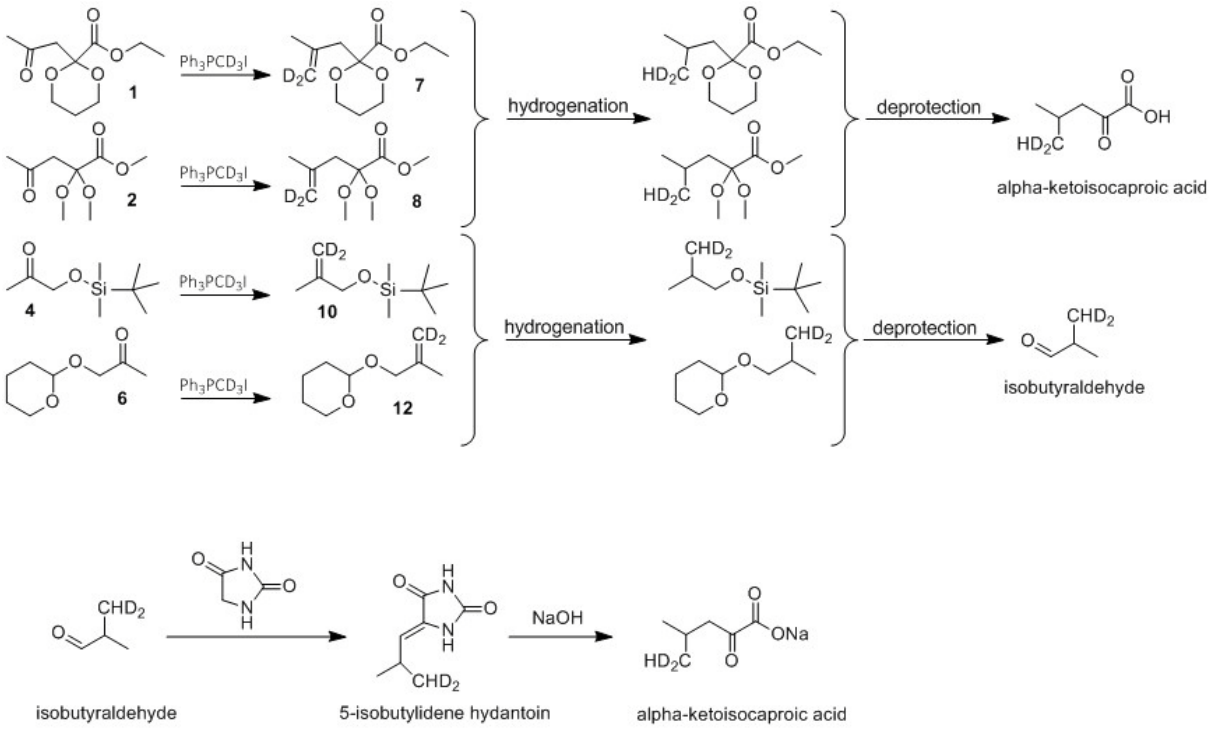

Figure 9: Synthetic route for α-ketoisocaproic acid starting from compound 1, 2, 4 or 6.

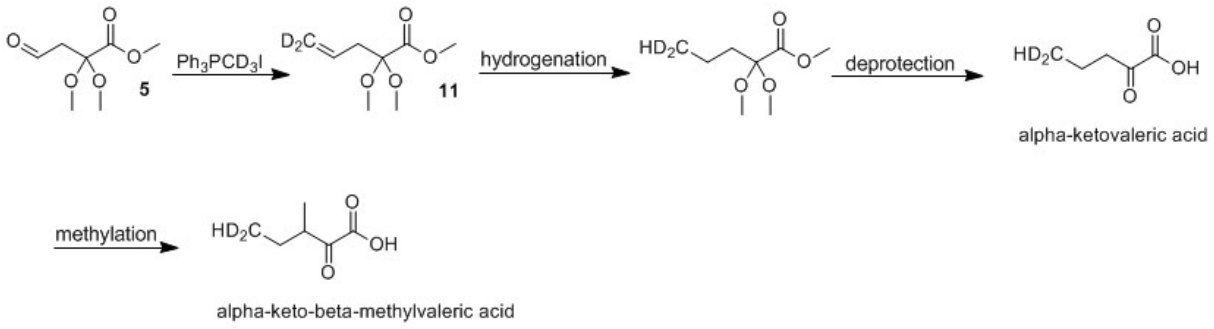

Figure 10: Synthetic route for α -keto-beta-methylvaleric acid starting from compound 5.

3 Results and Discussion

For a better understanding of this chapter it has to be anticipated that the first reaction step of the synthetic route (the Wittig Reaction) proved to be so challenging that only one of the six tested reactants, namely 1-(tetrahydropyran-2-yloxy)-2-propanone (6), reached the second reaction step. The other reactants were thoroughly processed by performing at least five replicates for each of many tested conditions, which are summarized in the following for each compound. However, they failed to proceed to the second reaction step. For compound 6 the Wittig as well as the subsequent hydrogenation reaction is described.

For the olefination of the compounds the Wittig Reaction was performed. The whole reaction was done under dry, inert conditions. The first step of the Wittig Reaction is the formation of the ylide, which is accomplished by adding a base to the solvated Wittig Salt. The successful formation of the methylene ylide is recognizable from a strong yellow colouring. Subsequently, the reactant is added, which changes the colour of the solution immediately to orange or brown.

The Wittig Reaction was first performed with 'unlabelled' reactants. In the cases where the olefination was successful deuterated Wittig Salt (Ph_3PCD_3I) was applied.

For the Wittig Reaction the quantity of the reactant was between 30 and 50 mg. Wittig Salt was used in 1.5- to 2.5-fold molar excess relative to the substrate. The base was added in an equivalent amount (mole) as the Wittig Salt.

3.1 Olefination of ethyl 4-oxo-2,2-(propylenedioxo)-pentanoate (1)

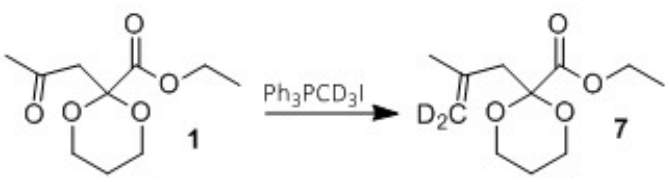

Figure 11: Olefination of compound 1 via the Wittig Reaction.

Table 4: Reaction conditions for the Wittig Reaction of ethyl 4-oxo-2,2-(propylenedioxo)-pentanoate and Ph_3PCH_3I.

Solvent	Base	Reaction condition		Reaction step
		Reaction time	Reaction temperature	
THF	NaHMDS	45 min	0 °C	Ylide formation[a]
		over night	-78 °C	Olefination[b]
THF	*n*-BuLi	30 min	- 40 °C	Ylide formation[a]
		1,0 h 3,5 h	- 40 °C 0 °C	Olefination[b]

[a] Ylide formation = base + Ph_3PCH_3I
[b] Olefination product= ethyl 4-methylidene-2,2-(propylenedioxo)-pentanoate

3.2 Olefination of methyl 2,2-dimethoxy-4-oxopentanoate (2)

Figure 12: Olefination of compound 2 via the Wittig Reaction.

Table 5: Reaction conditions for the Wittig Reaction of methyl 2,2-dimethoxy-4-oxopentanoate and Ph_3PCH_3I.

Solvent	Base	Reaction condition		Reaction step
		Reaction time	Reaction temperature	
THF	NaHMDS	45 min	0 °C	Ylide formation[a]
		over night	-78 °C	Olefination[b]
THF	*n*-BuLi	40 min	- 40 °C	Ylide formation[a]
		1 h 3 h	- 40 °C 0 °C	Olefination[b]
Diethyl ether	NaHMDS	45 min	0 °C	Ylide formation[a]
		over night	-78 °C	Olefination[b]
Diethyl ether	*n*-BuLi	1 h	- 20 °C	Ylide formation[a]
		1 h 4 h	rt 30 °C	Olefination[b]
THF	*n*-BuLi	1 h	-70 °C	Ylide formation[a]

		1 h 3 h	- 30 °C 0 °C	Olefination[b]
THF	*n*-BuLi	50 min	- 60 °C	Ylide formation[a]
		1 h 4 h	- 35 °C - 35 °C ↦ rt reflux	Olefination[b]
THF	*t*-BuOK	1 h	rt	Ylide formation[a]
		4 h	rt	Olefination[b]

[a] Ylide formation = base + Ph_3PCH_3I

[b] Olefination product= methyl 2,2-dimethoxy-4-methylidene-pentanoate

3.3 Olefination of 4,4-Dimethoxy-2-butanone (3)

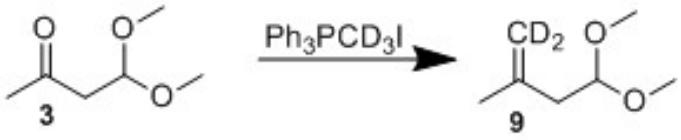

Figure 13: Olefination of compound 3 via the Wittig Reaction.

Table 6: Reaction conditions for the Wittig Reaction of 4,4-Dimethoxy-2-butanone and Ph_3PCH_3I.

Solvent	Base	Reaction condition		Reaction step
		Reaction time	Reaction temperature	
THF	*n*-BuLi	1 h	- 70 °C	Ylide formation[a]
		3 h	- 10 °C	Olefination[b]
THF	*t*-BuOK	1 h	rt	Ylide formation[a]
		3 h	rt	Olefination[b]
THF	*n*-BuLi	1 h	-60 °C	Ylide formation[a]
		3 h	-30 °C	Olefination[b]
Toluene	*t*-BuOK	1,5 h	45 °C	Ylide formation[a]
		4 h	40 °C	Olefination[b]
DMSO	*t*-BuOK	1,5 h	30 °C	Ylide formation[a]
		4 h	30 °C	Olefination[b]
THF	*n*-BuLi	1 h	0 °C	Ylide formation[a]
		3 h	rt	Olefination[b]

THF	*t*-BuOK	1 h	rt	Ylide formation[a]
		4 h	30 °C	Olefination[b]

[a] Ylide formation = base + Ph_3PCH_3I
[b] Olefination product = 4,4-dimethoxy-2-methylbut-1-ene

3.4 Olefination of 3-((*tert*-butyldimethylsilyl)oxo)-2-propanone (4)

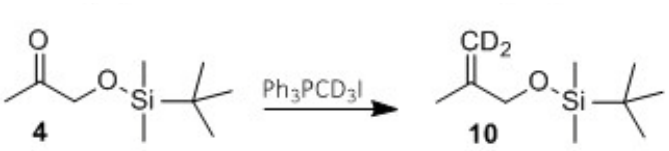

Figure 14: Olefination of compound 4 via the Wittig Reaction.

Table 7: Reaction conditions for the Wittig Reaction of 3-((*tert*-butyldimethylsilyl)oxo)-2-propanone and Ph_3PCH_3I.

Solvent	Base	Reaction condition		Reaction step
		Reaction time	Reaction temperature	
THF	*t*-BuOK	1 h	rt	Ylide formation[a]
		2 h	rt	Olefination[b]
Toluene	*t*-BuOK	45 min	55 °C	Ylide formation[a]
		3 h	45 °C	Olefination[b]
THF	*t*-BuOK	45 min	30 °C	Ylide formation[a]
		3 h	30 °C	Olefination[b]
THF	*t*-BuOK	45 min	30 °C	Ylide formation[a]
		4,5 h	30 °C	Olefination[b]
THF	*t*-BuOK	30 min	rt	Ylide formation[a]
		2,5 h	rt	Olefination[b]
THF	*t*-BuOK	1 h	rt	Ylide formation[a]
		4 h	rt	Olefination[b]
THF	*t*-BuOK	1 h	rt	Ylide formation[a]

		7 h	rt	Olefination[b]
DMF	*t*-BuOK	1,5 h	rt	Ylide formation[a]
		3,5 h	rt	Olefination[b]

[a] Ylide formation = base + Ph_3PCH_3I

[b] Olefination product = 2-methyl-3-((*tert*-butyldimethylsilyl)oxo)-prop-1-ene

For the following reaction condition the substrate was partially converted into 2-methyl-3-((*tert*-butyldimethylsilyl)oxo)-prop-1-ene:

Table 8: Reaction condition that led to a partial olefination of 3-((*tert*-butyldimethylsilyl)oxo)-2-propanone.

Solvent	Base	Reaction condition		Reaction step
		Reaction time	Reaction temperature	
THF	*t*-BuOK	1 h	rt	Ylide formation[a]
		over night	rt	Olefination[b]

The ratio of substrate to product (derived from the NMR spectrum) was 10 : 1. This result could not be reproduced.

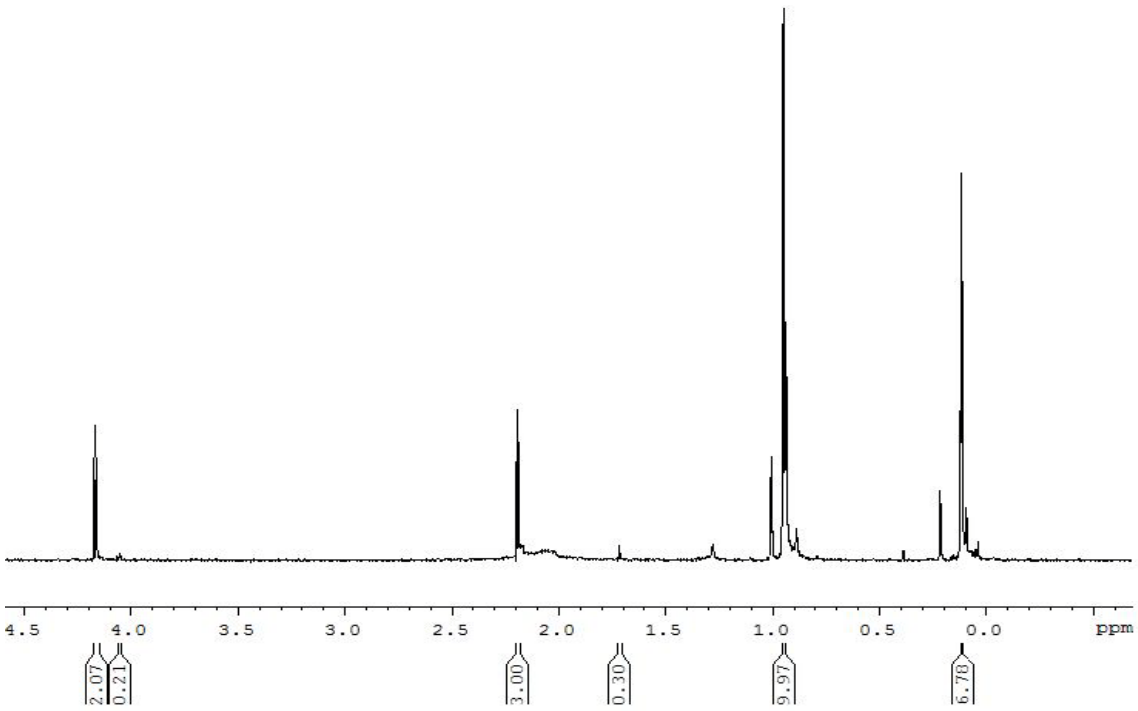

Figure 15: ^{1}H-spectrum of olefinated and partially deuterated compound 4.

3.5 Olefination of methyl 2,2-dimethoxy-4-oxobutanoate (5)

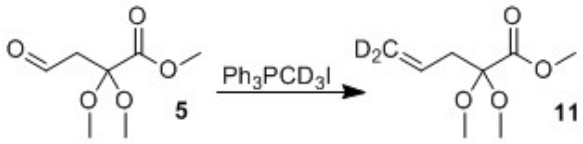

Figure 16: Olefination of compound 5 via the Wittig Reaction.

Table 9: Reaction conditions for the Wittig Reaction of methyl 2,2-dimethoxy-4-oxobutanoate and Ph_3PCH_3I.

Solvent	Base	Reaction condition		Reaction step	Ratio substrate/product
		Reaction time	Reaction temperature		
THF	NaHMDS	45 min	0 °C	Ylide formation[a]	-
		over night	- 78 °C	Olefination[b]	
THF	*n*-BuLi	30 min	-30 °C	Ylide formation[a]	-
		1,3 h 2,6 h	-30 °C 0 °C	Olefination[b]	
THF	*t*-BuOK	1 h	rt	Ylide formation[a]	-
		3 h	rt	Olefination[b]	
THF	*t*-BuOK	25 min	rt	Ylide formation[a]	-
		3,5 h	0 °C	Olefination[b]	
THF	*n*-BuLi	50 min	-50 °C	Ylide formation[a]	-
		over night	rt	Olefination[b]	
THF	*t*-BuOK	1 h	rt	Ylide formation[a]	1:2
		4 h	30 °C	Olefination[b]	
THF	*t*-BuOK	1 h	rt	Ylide formation[a]	1:6
		5 h	35 °C	Olefination[b]	
THF	*t*-BuOK	1 h	rt	Ylide formation[a]	-

		5 h	reflux	Olefination[b]	
DMSO	*t*-BuOK	1 h	rt	Ylide formation[a]	-
		1 h	35 °C	Olefination[b]	
DMSO	*t*-BuOK	1 h	30 °C	Ylide formation[a]	-
		4 h	30 °C	Olefination[b]	
Toluene	*t*-BuOK	25 min	50 °C	Ylide formation[a]	Completely converted
		3 h	35 °C	Olefination[b]	

[a] Ylide formation = base + Ph_3PCH_3I

[b] Olefination product = methyl 2,2-dimethoxy-4-methylene-butanoate

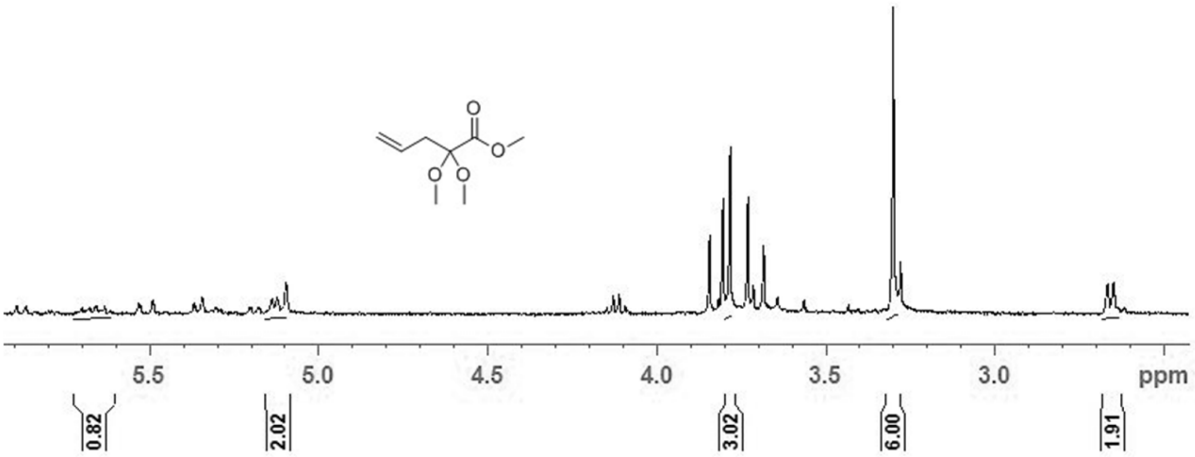

Figure 17: ^{1}H-spectrum of olefinated compound 5.

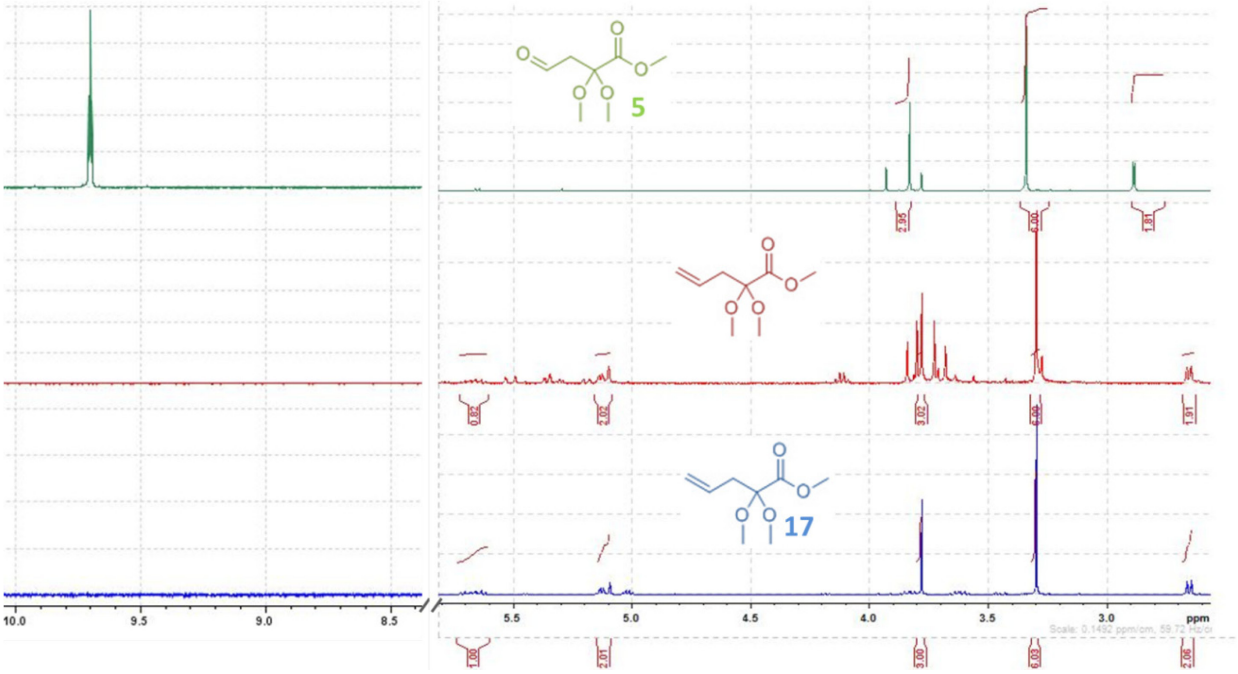

Figure 18: Comparison of ^{1}H-spectra. The red spectrum shows the olefination product of compound 5 via the Wittig Reaction. The comparison with the spectrum of compound 5 (green) shows that the additional peaks do not belong to the educt. The blue spectrum shows compound 17, which is also methyl 2,2-dimethoxy-4-methylene-butanoate, but synthesized via a different reaction pathway (see experimental section).

After the successful reaction of methyl 2,2-dimethoxy-4-oxobutanoate with Ph_3PCH_3I, it was tried to repeat the reaction with Ph_3PCD_3I under the same condition. This attempt failed. Therefore, other reaction conditions were tested (Table 10).

Table 10: Reaction conditions for the Wittig Reaction of methyl 2,2-dimethoxy-4-oxobutanoate and Ph_3PCD_3I.

Solvent	Base	Reaction condition		Reaction step
		Reaction time	Reaction temperature	
THF	*t*-BuOK	25 min 15 min	rt 37 °C	Ylide formation[a]
		3 h	35 °C	Olefination[b]
THF	*t*-BuOK	5 min	37 °C	Ylide formation[a]
		3 h	35 °C	Olefination[b]
Toluene	*t*-BuOK	30 min	50 °C	Ylide formation[a]
		3 h	rt	Olefination[b]
Toluene	*t*-BuOK	10 min 20 min	30 °C 40 °C	Ylide formation[a]
		3 h	30 °C	Olefination[b]
DMSO	*t*-BuOK	30 min	35 °C	Ylide formation[a]

		3 h	30 °C	Olefination[b]
THF	*t*-BuOK	40 min	26 °C	Ylide formation[a]
		3,5 h	26 °C	Olefination[b]
Toluene	*t*-BuOK	30 min	45 °C	Ylide formation[a]
		3 h	30 °C	Olefination[b]
Toluene	*t*-BuOK	30 min	45 °C	Ylide formation[a]
		4,5 h	30 °C	Olefination[b]

[a] Ylide formation = base + Ph_3PCD_3I

[b] Olefination product = methyl 2,2-dimethoxy-4-(methylene-D_2)-butanoate

The following condition led to a partial deuteration:

Table 11: Reaction condition that led to a partial deuteration of methyl 2,2-dimethoxy-4-(methylene-D_2)-butanoate.

Solvent	Base	Reaction condition		Reaction step
		Reaction time	Reaction temperature	
THF	*t*-BuOK	1 h	rt	Ylide formation[a]
		3 h	rt	Olefination[b]

[a] Ylide formation = base + Ph_3PCD_3I

[b] Olefination product = methyl 2,2-dimethoxy-4-(methylene-D_2)-butanoate

The comparison of the NMR spectra of the product of the Wittig Reaction with the spectra of the substrate and the 'non-deuterated' Wittig Reaction product showed that the introduced methylene group as well as the C_3-methylene group were only half deuterated (Figure 19). Proton exchange is a possible explanation for this observation. It was therefore considered to first introduce deuterium at the C_3-position of methyl 2,2-dimethoxy-4-oxobutanoate and then perform the Wittig Reaction with [3,3-D_2]-methyl-2,2-dimethoxy-4-oxobutanoate and Ph_3PCD_3I.

Methyl 2,2-dimethoxy-4-oxobutanoate was dissolved under argon atmosphere in THF and D_2O. After the addition of freshly distilled triethylamine the solution was stirred at room temperature for 1,5 hours and subsequently neutralized by the addition of D_2SO_4. Since this procedure did not achieve the desired result, the reaction time and temperature were varied. After several different reaction conditions were tested without any success, further attempts were ceased.

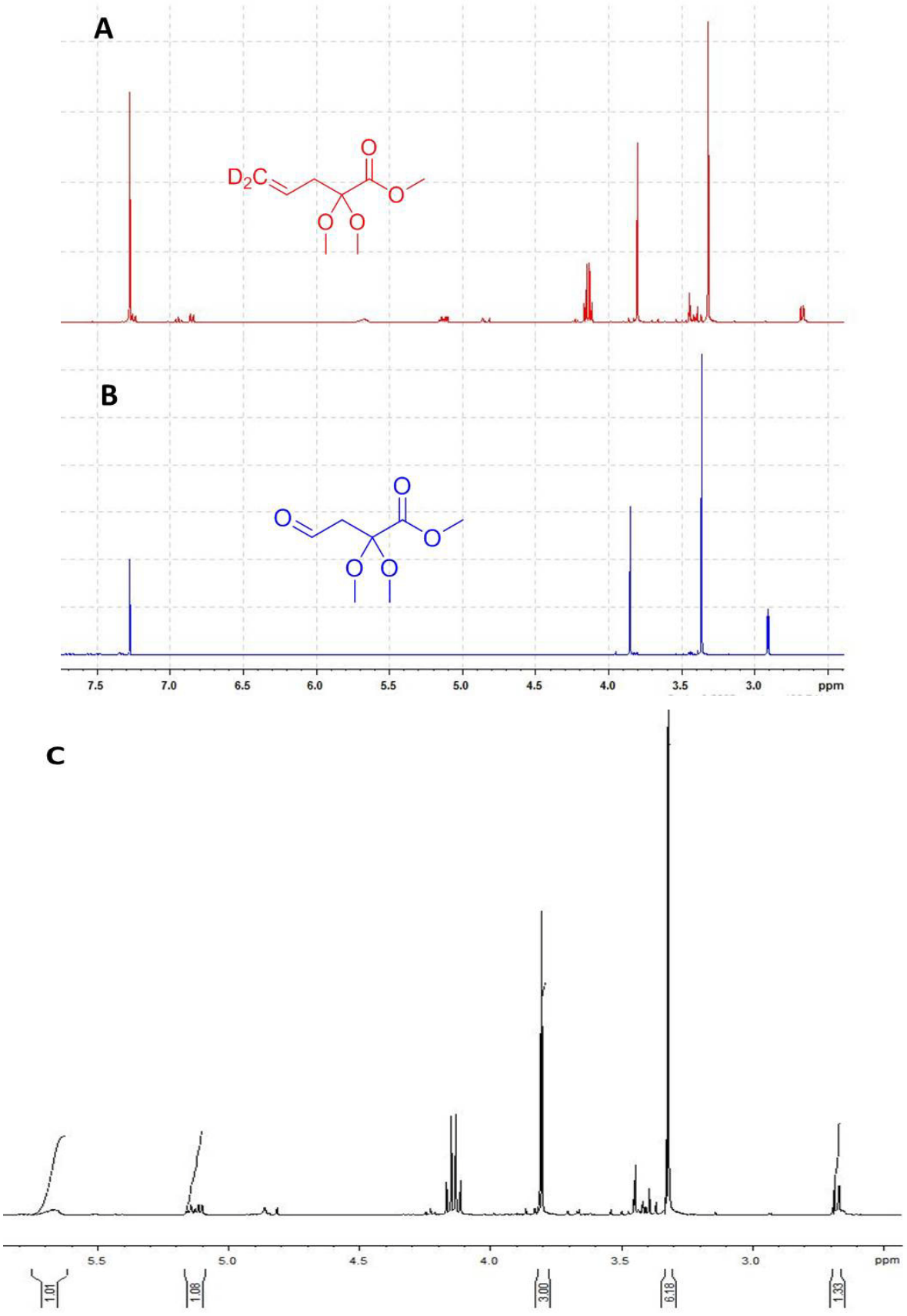

Figure 19: NMR spectra of the product of the Wittig Reaction (spectrum A), of methyl 2,2-dimethoxy-4-oxobutanoate (spectrum B) and an enlarged excerpt of spectrum B (spectrum C).

3.6 1-(tetrahydropyran-2-yloxy)-2-propanone (6)

3.6.1 Olefination of 1-(tetrahydropyran-2-yloxy)-2-propanone (6)

Figure 20: Olefination of compound 6 via the Wittig Reaction.

Table 12: Reaction conditions for the Wittig Reaction of 1-(tetrahydropyran-2-yloxy)-2-propanone and Ph_3PCH_3I.

Solvent	Base	Reaction condition		Reaction step	Ratio substrate/product
		Reaction time	Reaction temperature		
THF	*t*-BuOK	1 h	rt	Ylide formation[a]	-
		6 h	rt	Olefination[b]	
THF	*n*-BuLi	50 min	-40 °C	Ylide formation[a]	-
		over night	0 °C ↦ rt	Olefination[b]	
DMF	*t*-BuOK	1,5 h	rt	Ylide formation[a]	-
		3 h	rt	Olefination[b]	
Toluene	*t*-BuOK	50 min	30 °C	Ylide formation[a]	-
		3 h	30 °C	Olefination[b]	
Diethyl ether	*n*-BuLi	50 min	-30 °C	Ylide formation[a]	-
		3 h	30 °C	Olefination[b]	
THF	LiHMDS	40 min	0 °C	Ylide formation[a]	2:1
		4 h	0 °C	Olefination[b]	
THF	NaHMDS	40 min	0 °C	Ylide formation[a]	1:1
		4 h	0 °C	Olefination[b]	
THF	LiHMDS	1 h	0 °C	Ylide formation[a]	1:10
		1 h 3,75 h	0 °C rt	Olefination[b]	
THF	LiHMDS	45 min	rt	Ylide formation[a]	1:10
		over night	rt	Olefination[b]	
THF	LiHMDS	1 h	rt	Ylide formation[a]	1:10
		4,75 h	0 °C	Olefination[b]	
THF	NaHMDS	40 min	0 °C	Ylide formation[a]	1:10
		4 h	0 °C ↦ 14 °C	Olefination[b]	
THF	LiHMDS	40 min	0 °C	Ylide formation[a]	1:20
		4 h	0 °C ↦ 14 °C	Olefination[b]	
THF	LiHMDS	45 min	0 °C	Ylide formation[a]	1:300
		over night	rt	Olefination[b]	
THF	LiHMDS	50 min	0 °C	Ylide formation[a]	complete conversion
		30 min 3.5 h	0 °C rt	Olefination[b]	

[a] Ylide formation = base + Ph_3PCH_3I

[b] Olefination product = 2-methyl(tetrahydropyran-2-yloxy)-prop-1-ene (12)

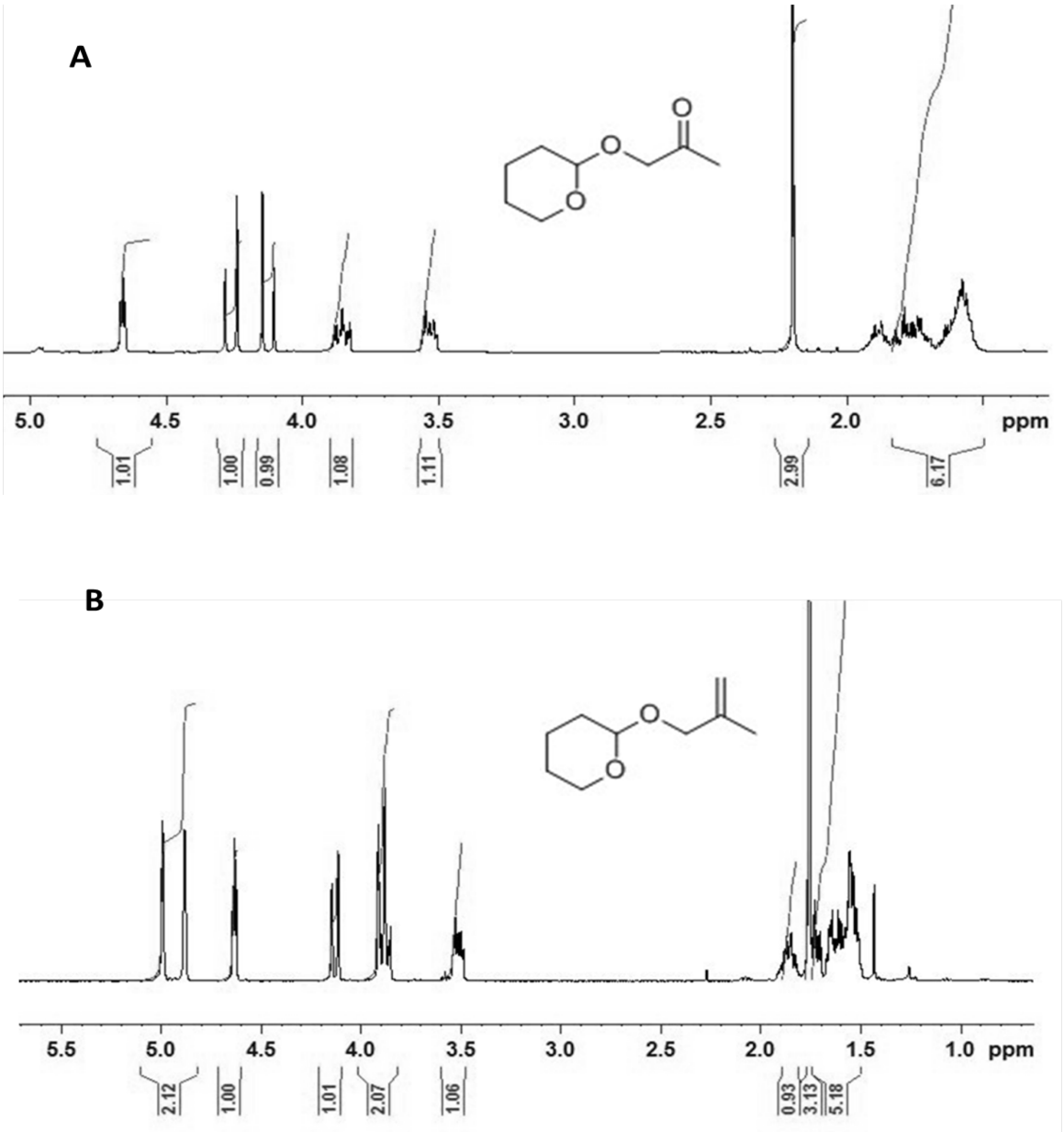

Figure 21: Comparison of ^{1}H-spectra of compound 6 (spectrum A) and its olefination product (spectrum B).

86 % deuteration of the methylene group was achieved applying the following reaction condition:

Table 13: Reaction condition that led to 86% deuteration of 2-methyl(tetrahydropyran-2-yloxy)-prop-1-ene (12).

Solvent	Base	Reaction condition		Reaction step
		Reaction time	Reaction temperature	
THF	LiHMDS	50 min	0 °C	Ylide formation[a]
		4.5 h	rt	Olefination[b]

[a] Ylide formation = base + Ph_3PCD_3I

[b] Olefination product = [1,1-D_2]-2-methyl(tetrahydropyran-2-yloxy)prop-1-ene (12)

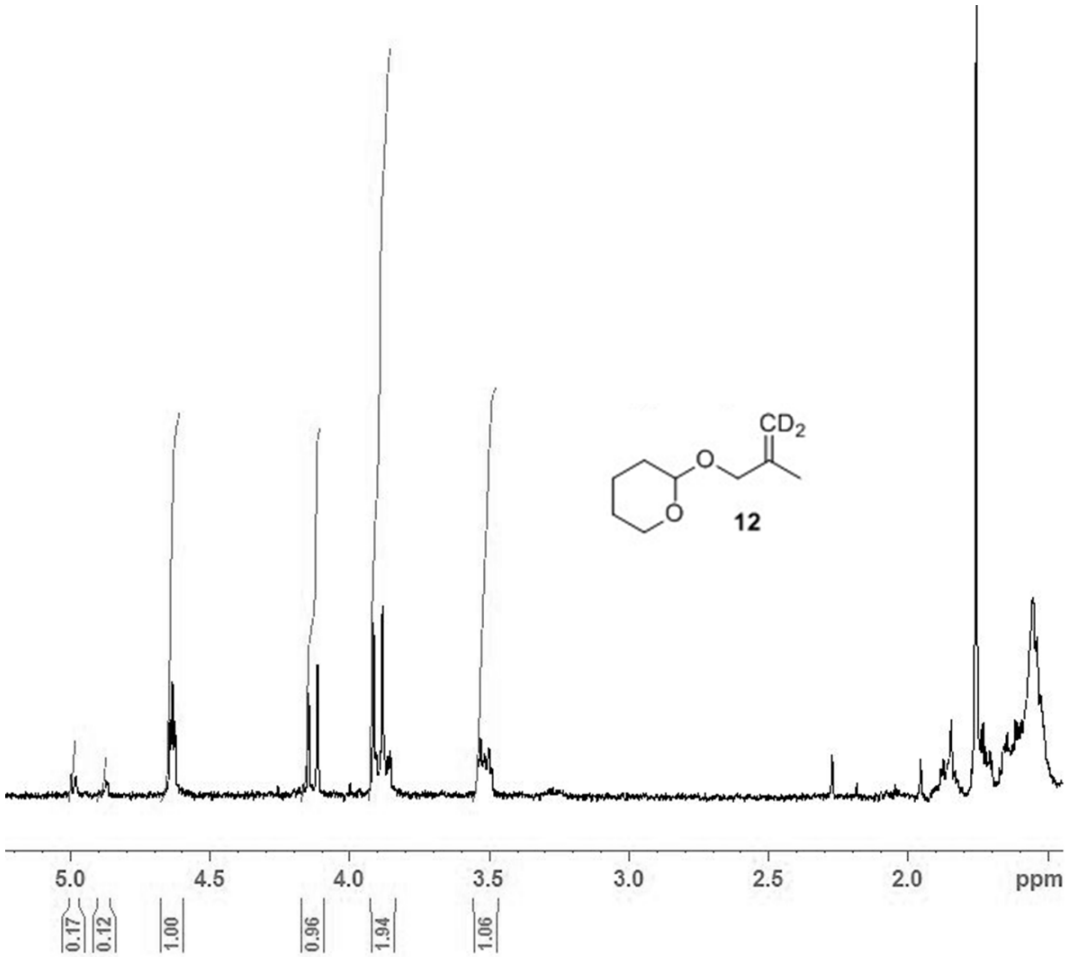

Figure 22: Olefination of compound 6 by deuterated Wittig Salt.

Deuteration of the alpha positions (C_1 and C_3) of 1-(tetrahydropyran-2-yloxy)-2-propanone (6) was attempted on the one hand to increase the degree of deuteration at the methylene group of 2-methyl(tetrahydropyran-2-yloxy)prop-1-ene (12) and on the other hand because of the improvement of the spectroscopic properties of the precursor. The following procedure yielded the highest deuteration level:

The substrate was dissolved in a 1:1 mixture of D_2O and 1,4-dioxane under argon atmosphere. After 0,1 equivalents of pyrrolidine were added, the solution was stirred for 4 hours at room temperature. The product was extracted with diethyl ether and dried over $MgSO_4$. After evaporation of diethyl ether, the product was purified by Kugelrohr distillation (110 °C; 10 Torr) to give the desired product in 76 % yield. The deuteration level of the C_3-methyl group and the C_1-methylene bridge accounted for 90 % and 92 %, respectively (figure 23).

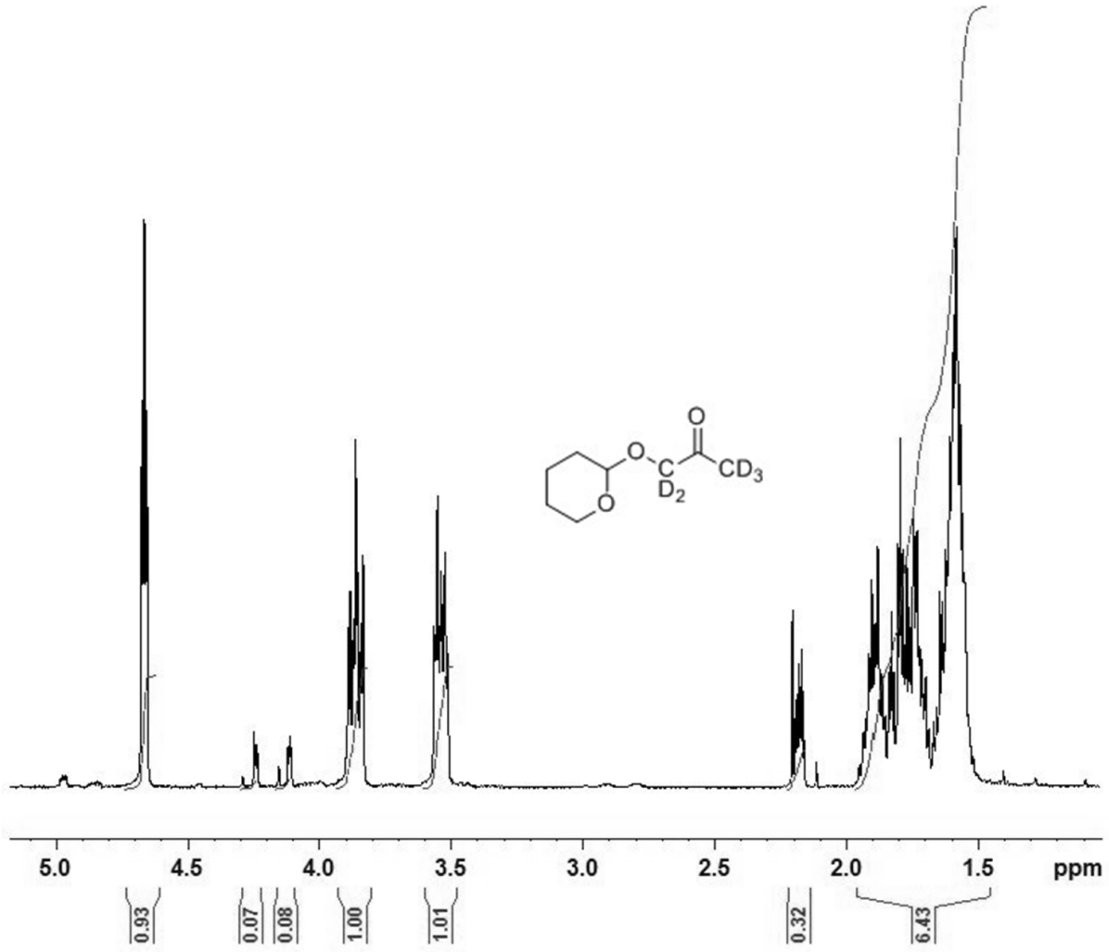

Figure 23: Deuteration of the alpha positions of compound 6.

Subsequently the Wittig Reaction was carried out with the deuterated 1-(tetrahydropyran-2-yloxy)-2-propanone under the condition listed in table 13. Ph_3PCD_3I and LiHMDS were each added in a 1,4-fold excess. The product was extracted with DCM and dried over $MgSO_4$. After the removal of the solvent by evaporation under reduced pressure, a Kugelrohr distillation (90 °C, 5 Torr) was performed to give the purified product in 23 % yield. The deuteration level of the methylene group amounted to 93 % (derived from ^{1}H-NMR spectrum) (figure 24).

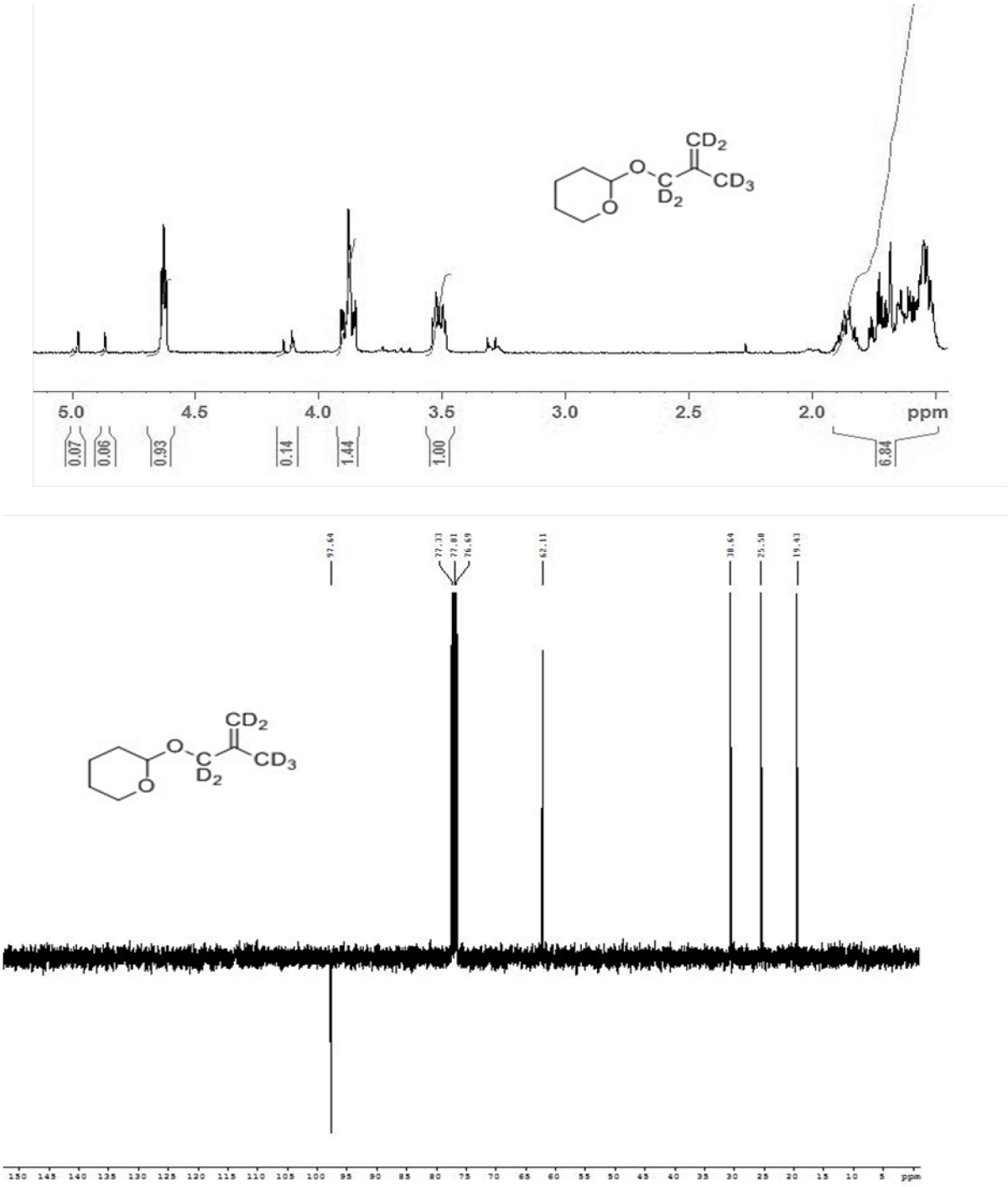

Figure 24: ^{1}H- and ^{13}C-spectrum of the product of the Wittig Reaction which was carried out with Ph_3PCD_3I and compound 6 deuterated at the alpha-positions.

3.6.2 Hydrogenation of 2-methyl(tetrahydropyran-2-yloxy)- prop-1-ene (12)

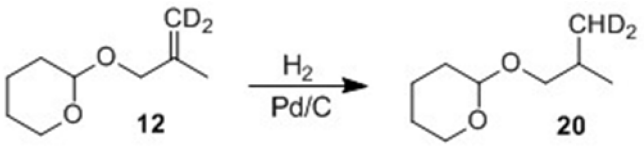

Figure 25: Hydrogenation of compound 12.

The Hydrogenation reaction was carried out with a ThalesNano H-Cube® Continuous Flow Hydrogenation Reactor equipped with a palladium on carbon (10 %) ThalesNano CatCart® Cartridge as a catalyst.

To determine the optimal reaction condition, the hydrogenation was first performed on the "unlabelled" reactant 2-methyl(tetrahydropyran-2-yloxy)- prop-1-ene. The following condition was found:

2-methyl(tetrahydropyran-2-yloxy)- prop-1-ene was dissolved in ethyl acetate to a concentration of 0,02 M and subjected to the H-Cube® at room temperature with a flow rate of 1 ml/min at "full H_2" stream. The hydrogenated product was collected and ethyl acetate was removed by evaporation under reduced pressure. The yield amounted to 35 % of 2-methyl(tetrahydropyran-2-yloxy)-propane (20).

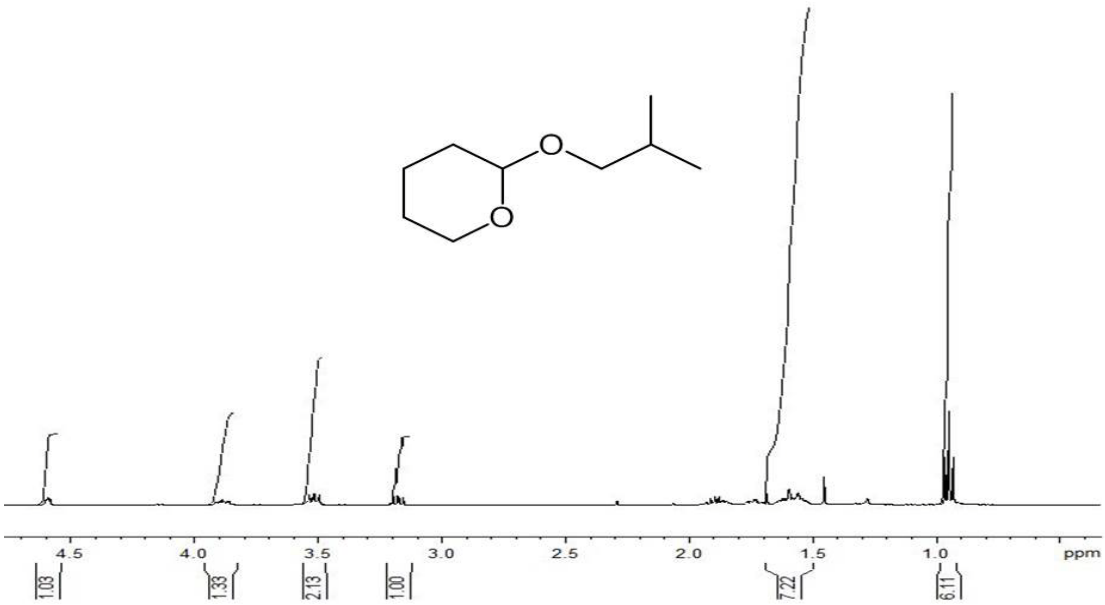

Figure 26: ^{1}H-spectrum of the hydrogenation product.

The reduction of 2-methyl(tetrahydropyran-2-yloxy)-prop-1-ene could not be reproduced with the deuterated substrate under the above mentioned conditions. Other reaction conditions have not been tested yet.

3.7 Concluding observations of the experimental procedure

The above listed tables only show the approaches that resulted in a NMR spectrum with assignable signals. But numerous reactions were interrupted when the ylide formation did not seem to take place. In several other cases the NMR spectrum revealed the degradation of the substrate. In the course of these many attempts every single step has been carefully scrutinised: beginning from the storage of the chemicals through the preparation of the equipment to the manner the Wittig Salt was added to the reaction mixture.

Major setbacks were the cases where the reaction conditions found for the 'unlabelled' substrate could not be adopted to its labelled counterpart presumably due to the unexpectedly high influence of isotope effects.

A significant and time consuming problem was the low yields of the substrate syntheses as this hindered the fluent work process.

An important observation was done towards the end of the practical work: the used *t*-BuOK did not possess full reactivity anymore. This was not recognized before because the same batch of *t*-BuOK was used in our laboratory for other reaction types for which the reduced reactivity was sufficient.

4 CONCLUSION AND OUTLOOK

Although, the objective of this master's thesis was not achieved, the successful introduction of a CD_2-methylene group into 1-(tetrahydropyran-2-yloxy)-2-propanone (6) represents an important step towards the aimed incorporation of a $^{13}CD_2H$-methyl group into the leucine precursor α-ketoisocaproate. This is especially true because the remaining reactions to complete the synthetic route are standard reactions that are frequently performed at our laboratory. The determination of the appropriate reaction conditions for the remaining reaction steps are therefore not expected to pose a major issue nor does the subsequent incorporation of ^{13}C via ^{13}C-labelled methyltriphenylphosphonium iodide.

In addition, it was found that methyl 2,2-dimethoxy-4-oxobutanoate (5) and 3-((*tert*-butyldimethylsilyl)oxo)-2-propanone (4) show a certain degree of reactivity for olefination via the Wittig Reaction and should be further pursued. In particular because of the above mentioned insufficient reactivity of *t*-BuOK.

Since the found reaction conditions for the 'unlabelled' substrates could so far not be adopted to the labelled substrates, the expedience of this approach should be questioned. It might be more economical in regard of time and costs to test the conditions directly on minor amounts of labelled substrate.

5 EXPERIMENTAL SECTION

5.1 General comments

All reagents and reactants were acquired by purchase and used without further purification. Solvents have been distilled. Dry solvents were stored over molecular sieves (4 Å) under argon atmosphere.

^1H and ^{13}C NMR spectra were recorded on a Bruker 400 MHz spectrometer. Chemical shift (δ) is given in parts per million (ppm) relative to tetramethylsilane. NMR data is indicated by chemical shift (δ), number of equivalent nuclei, multiplicity (s = singlet, d = doublet, dd = doublet of doublets, t = triplet, q = quartet, m = multiplet) and coupling constants (*J*) in Hertz

(Hz). NMR spectra were measured in $CDCl_3$. The signal of $CDCl_3$ was calibrated to 7.26 ppm. For flash chromatographies Merck silica gel 60 (0.004-0.063 mm) was used.
All reactions mixtures (except for reactions performed in the microwave reactor) were stirred by a magnetic stirrer with magnetic stir bars. Reaction progress was monitored by TLC on Macherey-Nagel ALUGRAM® TLC-sheets (0,20 mm, silica gel 60, fluorescent indicator UV_{254}); visualization of the spots was achieved by an UV-lamp (254 nm) or by heating the TLC-sheet with a heat gun after staining with a cerium molybdate solution ($(NH_4)_6Mo_7O_{24} \cdot 4\ H_2O$ (48 g) and $Ce(SO_4)_2$ (2 g) in 10 % H_2SO_4 (1 L)), followed by heating.
Microwave reactions were performed on a Biotage® Initiator+ Microwave Synthesizer.
Ozonolysis was performed by using an Anseros® Ozone Generator COM-AD-04 and an Anseros® Oxygen Generator SEP-100.

5.2 Synthetic protocols

In the following the synthetic protocols of compound 1, 2, 5, 6 and [D_3]-methyltriphenylphosphonium iodide are listed. 3-((*tert*-butyldimethylsilyl)oxo)-2-propanone (4) was kindly provided by Dr. Roman Lichtenecker. 4,4-Dimethoxy-2-butanone (3) was purchased from Alfa Aesar (Thermo Fisher Scientific).

5.2.1 Ethyl 4-oxo-2,2-(propylenedioxo)-pentanoate (1)

Ethyl 1,3-dioxane-2-carboxylate (13)

Synthetic protocol modified from literature.[71]

A three-necked flask was evacuated, set under argon and equipped with a reflux condenser and a septum. Boron trifluoride etherate (5.8 ml, 45.0 mmol) and dry chloroform (14.0 ml) were added through a syringe. The solution was heated to reflux. A solution of ethyl diethoxyacetate (4.0 ml, 22.4 mmol), 1,3-propanediole (1.6 ml, 22.6 mmol) and dry chloroform (4.0 ml) was added with a syringe over a period of 15 minutes. The solution was stirred for 40 minutes at reflux. After allowing the mixture to come to room temperature, it was washed with water, aqueous potassium carbonate (10 %), water and brine. The organic phase was dried over $MgSO_4$. After filtration, the solvents were removed *in vacuo* to

yield a yellowish liquid which was purified by micro-distillation (104 °C / 6 Torr) to give a colourless liquid. 1.160 g ethyl 1,3-dioxane-2-carboxylate (7) (7.2 mmol, 32 %) was obtained.

^{1}H NMR (400.3 MHz, $CDCl_3$): δ= 5.01 (s, 1H), 4.27 (q, ^{3}J= 7.16 Hz, 2H), 4.25-4.20 (m, 2H), 3.90-3.82 (m, 2H), 2.24-2.11 (m, 1H), 1.47-1.40 (m, 1H), 1.31 (t, ^{3}J= 7.13 Hz, 3H).
^{13}C (100.6 MHz, $CDCl_3$): δ= 166.01 (CH**C**OO), 96.61 (**C**H), 67.07 (2x CH_2**C**H_2O), 61.87 (CH_3**C**H_2), 25.35 (CH_2**C**H_2CH_2), 14.02 (**C**H_3).

Ethyl 4-methylidene-2,2-(propylenedioxo)-pentanoate (14)

Synthetic protocol modified from literature.[72]

2 M LDA (800 µl, 1.6 mmol) and dry THF (1.8 ml) were added to a two-necked flask, which was evacuated, set under argon and equipped with a septum and an adapter with stopcock connected to an argon reservoir. The solution was cooled to -78 °C and ethyl 1,3-dioxane-2-carboxylate (13) (225 mg, 1.4 mmol) was added dropwise with a syringe. The solution was stirred for 30 minutes at 0 °C and was then again cooled to -78 °C. After the dropwise addition of 3-bromo-2-methylpropene (186 µl, 1.8 mmol), the solution was warmed to 0 °C and stirred for 3 hours. The reaction was stopped by adding 1 M HCl (5 ml) and diethyl ether (5 ml). The aqueous phase was extracted three times with diethyl ether. The organic extracts were combined, washed with saturated aqueous sodium bicarbonate solution and brine and dried over $MgSO_4$. Evaporation of the solvents gave a yellow liquid that was purified on a silica gel column using ethyl acetate/hexane 1:5 (v/v) as eluent. The product fractions were identified using TLC (R_f = 0.48). Evaporation of the solvents under reduced pressure yielded 65 mg ethyl 4-methylidene-2,2-(propylenedioxo)-pentanoate (14) (0.30 mmol, 22 %) as a colourless liquid.

^{1}H NMR (400.3 MHz, $CDCl_3$): δ=4.86-4.82 (m, 1H), 4.75-4.71 (m, 1H), 4.27 (q, ^{3}J=7.13 Hz, 2H), 4.04-3.83 (m, 4H), 2.53-2.48 (m, 2H), 2.17-2.04 (m, 1H), 1.84-1.79 (m, 3H), 1.38-1.35 (m, 1H), 1.33 (t, ^{3}J=7.14 Hz, 3H).

^{13}C (100.6 MHz, CDCl3): δ= 169.61 (**C**OO), 139.82 (CH_3**C**CH_2), 115.40 (CH_3**C**CH_2), 100.68 (CH_2**C**CO), 63.03 (**C**H_2CH_2**C**H_2), 61.36 (CH_3**C**H_2), 47.49 (**C**CH_2), 24.61 (CH_2**C**H_2CH_2), 23.53 (**C**H_3C), 14.33 (**C**H_3CH_2).

Ethyl 4-oxo-2,2-(propylenedioxo)-pentanoate (1)

A three-necked flask was evacuated, set under argon and equipped with a septum and two adapters with screw thread and silicone seal. Through these adapters two tubes got connected with the flask for gas in- and outlet. Ethyl 4-methylidene-2,2-(propylenedioxo)-pentanoate (14) (103 mg, 0.48 mmol) and dry chloroform (40 ml) were put into the flask using a syringe. The septum was replaced by a glass stopper. The solution was cooled to -78 °C and ozone (percentage of ozone in the air stream: 80 %) was bubbled through the mixture until its colour turned blue. Ozone was turned off so that only dry air bubbled through the solution. After the solution turned colourless again, triphenylphosphine (189 mg, 0.72 mmol) was added and the mixture was allowed to warm to room temperature. The flask was connected to an argon reservoir and stirred overnight at room temperature. The solvent was removed under reduced pressure to yield a colourless liquid that was purified via Kugelrohr distillation (120 °C, 7 Torr). 73 mg of ethyl 4-oxo-2,2-(propylenedioxo)-pentanoate (1) (0.34 mmol, 71 %) was obtained as a colourless liquid.

^{1}H NMR (400.3 MHz, $CDCl_3$): δ= 4.33 (q, ^3J=7.13, 2H), 4.04-3.96 (m, 4H), 2.88 (s, 2H), 2.24 (s, 3H), 2.15-2.04 (m, 1H), 1.43-1.36 (1H), 1.34 (t, ^3J=7.14, 3H).
^{13}C (100.6 MHz, CDCl3): δ= 62.92 (2x **C**H_2CH_2**C**H_2), 61.82 (**C**H_2CH_3), 52.74 (**C**CH_2), 31.64 (**C**H_2CO), 24.48 (CH_2**C**H_2CH_2), 14.18 (CH_2**C**H_3).

5.2.2 Methyl 2,2-dimethoxy-4-oxopentanoate (2)

Methyl 2,2-dimethoxyacetate (15)

Synthetic protocol modified from literature.[73]

Glyoxylic acid monohydrate (8.08 g, 88 mmol), *p*-toluenesulfonic acid monohydrate (1.48 g, 7.8 mmol) and trimethoxymethane (37.4 ml, 364 mmol) were added to a round bottom flask and stirred for 75 hours at room temperature. After the addition of saturated aqueous sodium bicarbonate solution (60 ml) and chloroform (60 ml), the aqueous phase was separated and extracted with chloroform (1x 50 ml, 2x 20 ml). The combined organic phases were dried over $MgSO_4$, filtered and evaporated to give 10.7 g methyl 2,2-dimethoxyacetate (15) as a colourless liquid (80 mmol, 91 %). No further purification was required.

^{1}H NMR (400.3 MHz, $CDCl_3$): δ= 4.81 (s, 1H), 3.80 (s, 3H), 3.42 (s, 6).

Methyl 2,2-dimethoxy-4-methylidene-pentanoate (16)

Synthetic protocol modified from literature.[72]

Tetramethylpiperidine (600 µl, 3.5 mmol) and dry THF (4.0 ml) were added to a two-necked flask, which was evacuated, set under argon and equipped with a septum and an adapter with stopcock connected to an argon reservoir. The solution was cooled to 0 °C and 2.5 M *n*-BuLi (1.5 ml, 3.5 mmol) was added dropwise with a syringe. After the solution was stirred for 20 minutes, it was cooled to -78 °C and methyl 2,2-dimethoxyacetate (15) (410 mg, 3.1 mmol) was added with a syringe over a period of 10 minutes. The amber-coloured solution was warmed to 0 °C, stirred for 30 minutes and then again cooled to -78 °C. After the dropwise addition of 3-bromo-2-methylpropene (405 µl, 4.0 mmol), the mixture was warmed to 0 °C and stirred for 3,5 hours. 1 M HCl (9 ml) and diethyl ether (9 ml) were added to stop the reaction. The layers were separated and the aqueous phase was extracted three times with diethyl ether. The combined organic extracts were washed with saturated aqueous sodium bicarbonate solution and brine and dried over $MgSO_4$. The dried solution was filtered and the solvents were evaporated under reduced pressure to give a light yellow liquid that was purified on a silica gel column using ethyl acetate/hexane 1:4 (v/v) as an eluent. The fractions that contained product were identified by TLC (R_f = 0.57). Evaporation of the solvents under reduced pressure yielded 108 mg methyl 2,2-dimethoxy-4-methylidene-pentanoate (16) (0.89 mmol, 29 %) as a colourless liquid.

^{1}H NMR (400.3 MHz, $CDCl_3$): δ= 4.86-4.81 (m, 1H), 4.80-4.75 (m, 1H), 3.76 (s, 3H), 3.30 (s, 6H),), 2.62 (d,^{4}J=0.89 Hz, 2H), 1.77-1-74 (m, 3H).
^{13}C (100.6 MHz, CDCl3): δ= 169.12 (**C**$OOCH_3$), 139.56 (CH_3**C**), 114.88 (CH_3**C**CH_2), 102.79 (CH_3**C**), 52.23 (COO**C**H_3), 49.86 (2x OCH_3), 41.64 (**C**H_2CO), 22.94 (**C**CH_3).

Methyl 2,2-dimethoxy-4-oxopentanoate (2)

In an evacuated three-necked flask, equipped with a septum and two adapters with screw thread and silicone seal, methyl 2,2-dimethoxy-4-methylidene-pentanoate (16) (168 mg, 0.89 mmol) was dissolved in dry chloroform (40 ml) under argon atmosphere. The flask was connected with two tubes for gas in- and outlet through the adapters. The septum was replaced by a glass stopper. After the solution was cooled to -78 °C, ozone (percentage of ozone in the air stream: 80 %) was bubbled through the liquid until it showed a blue colour. Dry air was passed through the solution until the solution turned colourless again. Triphenylphosphine (350 mg, 1.34 mmol) was added and after the reaction mixture had come to room temperature, it was stirred overnight at room temperature under argon atmosphere. The solvent was evaporated under reduced pressure to yield a colourless liquid that was purified via Kugelrohr distillation (135 °C, 2 Torr). 109 mg of Methyl 2,2-dimethoxy-4-oxopentanoate (2) (0.57 mmol, 64 %) was obtained as a colourless liquid.

^{1}H NMR (400.3 MHz, $CDCl_3$): δ= 3.82 (s, 3H), 3.29 (s, 6H), 3.10 (s, 2H), 2.17 (s, 3H).

5.2.3 Methyl 2,2-dimethoxy-4-oxobutanoate (5)

Methyl 2,2-dimethoxy-4-methylene-butanoate (17)

Synthetic protocol modified from literature.[72]

A two-necked flask was evacuated, set under argon and equipped with a septum and an adapter connected to an argon reservoir. Tetramethylpiperidine (650 µl, 3.9 mmol) and dry THF (4.0 ml) were added with a syringe. The solution was cooled to 0 °C and 2.5 M *n*-

BuLi (1.5 ml, 3.8 mmol) was added drop wise. After the solution was stirred for 20 minutes, it was cooled to -78 °C and methyl 2,2-dimethoxyacetate (15) (410 mg, 3.1 mmol) was added with a syringe within 10 minutes. The reaction mixture was stirred for 30 minutes at 0 °C and subsequently cooled to -78 °C. After the dropwise addition of 3-bromo-1-propene (376 µl, 4.3 mmol), the mixture was warmed to 0 °C and stirred for 4,5 hours. The reaction was stopped by the addition of 1 M HCl (9 ml) and diethyl ether (9 ml). The aqueous phase was separated and extracted three times with diethyl ether. The combined organic phases were washed with saturated aqueous sodium bicarbonate solution and brine. After drying over $MgSO_4$, the solution was filtered and the solvents were evaporated under reduced pressure to yield a yellow liquid, which was purified on a silica gel column using ethyl acetate/hexane 1:4 (v/v) as an eluent. TLC was used to detect the product containing fractions (R_f = 0.40). The solvents were evaporated under reduced pressure. 187 mg methyl 2,2-dimethoxy-4-methylene-butanoate (17) (1.07 mmol, 35 %) as a pale yellow liquid were obtained.

^{1}H NMR (400.3 MHz, $CDCl_3$): δ= 5.74-5.60 (m, 1H), 5.15-5.09 (m, 2H), 3.78 (s, 3H), 3.30 (s, 6H), 2.66 (dt, ^3J=7.19 Hz, ^4J=1.30 Hz, 2H).

Methyl 2,2-dimethoxy-4-oxobutanoate (5)

A three-necked flask was evacuated, set under argon and equipped with a septum and two tubes for gas in- and outlet. Methyl 2,2-dimethoxy-4-methylene-butanoate (17) (91 mg, 0.52 mmol) was filled into the flask by a syringe along with dry chloroform (40 ml). The septum was replaced by a glass stopper. The solution was cooled to -78 °C and ozone (percentage of ozone in the air stream: 80 %) was passed through the reaction mixture until it turned blue. Ozone was turned off and dry air was bubbled through the solution until the blue colour vanished. Triphenylphosphine (205 mg, 0.78 mmol) was added and the mixture was allowed to warm to room temperature. The solution was stirred overnight at room temperature and under argon atmosphere. The solvent was removed under reduced pressure to yield a colourless liquid that was purified via Kugelrohr distillation (110 °C, 4 Torr). 71 mg of methyl 2,2-dimethoxy-4-oxobutanoate (0.40 mmol, 77 %) were obtained as a colourless liquid.

^{1}H NMR (400.3 MHz, $CDCl_3$): δ= 9.70 (t, ^{3}J=2.58 Hz, 1H), 3.83 (s,3H), 3.34 (s, 6H), 2.89 (d, ^{3}J=2.56 Hz, 2H).
^{13}C (100.6 MHz, CDCl3): δ= 197.97 (**C**HO), 52.87 (COO**C**H_3), 50.30 (2x O**C**H_3), 47.46 (CH**C**H_2).

5.2.4 1-(tetrahydropyran-2-yloxy)-2-propanone (6)

Synthetic protocol modified from literature.[74]

A two-necked flask was evacuated, set under argon and equipped with a septum. Montmorillonite K-10 Clay (2g) was put into the flask along with dry DCM (40 ml) and 1-hydroxy-2-propanone (5.4 ml, 78.9 mmol) which were added with a syringe. While the solution was stirred at room temperature, 3,4-Dihydro-*2H*-pyran (10.8 ml, 118.4 mmol) was added over a period of 35 minutes. After the reaction mixture was stirred for 1 hour at room temperature, Montmorillonite K-10 Clay was filtered off and the solvents were evaporated *in vacuo*. A Kugelrohr distillation (86 °C, 4 Torr) was performed to purify the obtained liquid. 9.46 g 1-(tetrahydropyran-2-yloxy)-2-prpanone (6) (59.8 mmol, 76 %) were yielded as a colourless liquid.

^{1}H NMR (400.3 MHz, $CDCl_3$): δ= 4.66 (t, ^{3}J= 3.6 Hz, 1H), 4.26 (d, ^{2}J=17.3 Hz, 1H), 4.12 (d, ^{2}J= 17.3 Hz, 1H), 3.90-3.82 (m, 1H), 3.57-3.49 (m, 1H), 2.19 (s, 3H), 1.84-1.49 (m, 6H).
^{13}C (100.6 MHz, CDCl3): δ= 206.73 (CH_3**C**O), 94.66 (**C**H), 72.35 (O**C**H_2CO), 62.38 (**C**H_2OCH), 30.29 (**C**H_2CH), 26.50 (CH_3), 25.28 (**C**H_2 CH_2O), 19.19 (**C**H_2 CH_2 CH).

5.2.5 [D_3]-methyltriphenylphosphonium iodide

Methyltriphenylphosphonium iodide (18)

Synthetic protocol modified from literature.[75]

In a round bottom flask triphenylphosphine (5.0 g, 19.1 mmol) was dissolved in toluene (11 ml). The flask was closed with a septum and iodomethane (1.9 g, 13.4 mmol) was added dropwise with a syringe. The solution was stirred over night at room temperature. A white solid was obtained that was filtered and washed with toluene and hexane. The solid was dried *in vacuo*. 5.182 g methyltriphenylphosphonium iodide (18) (12.7 mmol, 95 %) was obtained as a white solid.

^{1}H NMR (400.3 MHz, $CDCl_3$): δ= 7.88 (m, 15H), 2.89 (d, ^{2}J=13.29 Hz, 3H).
^{13}C (100.6 MHz, CDCl3): δ= 135.21 (d, ^{4}J=3.04 Hz, *p*-**C**$_{arom.}$), 133.39 (d, ^{3}J=10.63 Hz, *m*-**C**$_{arom.}$), 130.51 (d, ^{2}J=12.80 Hz, *o*-**C**$_{arom}$), 119.05 (d, ^{1}J=88.74 Hz, *o*-**C**$_{arom}$),11.88 (d, ^{1}J=56.95 Hz, **C**H_3).

[D_3]-methyltriphenylphosphonium iodide (19)

Synthetic protocol modified from literature.[76]

Methyltriphenylphosphonium iodide (500 mg, 1.2 mmol), D_2O (3.2 ml) and several molecular sieves (3 Å) were added to a microwave glass vial. The vial was sealed with an appendant cap. The vial was put into the microwave reactor and heated to 180 °C for 30 minutes. After the vial was cooled to room temperature, the supernatant liquid was decanted and the remaining solid was dissolved in DCM. The molecular sieves were washed with DCM. The organic phases were combined, dried over $MgSO_4$ and filtered. The solution was evaporated to a few millilitres and ethyl acetate was added to precipitate the product. The solvents were removed by evaporation under reduced pressure. The solid was dried *in vacuo* to give quantitatively deuterated 429 mg [D_3]-methyltriphenylphosphonium iodide (19) (1.1 mmol, 85 %).

^{1}H NMR (400.3 MHz, $CDCl_3$): δ= 7.88-7.66 (m, 15H).

6 APPENDIX

6.1 Abstract

NMR spectroscopy plays an indispensable role in protein function studies since it represents the only method to elucidate both the protein's structure and its dynamics at atomic level under native like conditions. The tremendous developments that protein NMR has experienced during the last decades have often been expedited by the design of new isotopic labelling strategies. Selective insertion of CD_2H-methyl groups into perdeuterated proteins has proved to be a valuable tool for the detection of dynamic data. Furthermore, methyl groups tend to be accumulated in hydrophobic cores and are therefore excellent probes for studies of protein-ligand interactions.

A well-established method for selective isotope labelling of proteins is the heterologous overexpression of the desired protein in engineered bacteria strains in the presence of a labelled amino acid precursor. The aim of this master's thesis was the development of a synthetic route for the production of CD_2H-methyl group bearing leucine and isoleucine precursors using inexpensive starting material.

As a leucine precursor α-ketoisocaproate was chosen, whereas for isoleucine α-keto-β-methylvalerate was selected. The first step of the synthetic route, which is the same for both precursors, is the introduction of a CD_2-methylene group via the Wittig Reaction. This first reaction step turned out to be such challenging that the subject of this thesis was confined to the determination of the appropriate reaction conditions for the Wittig Reaction. For 1-(tetrahydropyran-2-yloxy)-2-propanone, the precursor of α-ketoisocaproate, a CD_2-methylene was successfully introduced.

6.2 Zusammenfassung

Für Proteinfunktionsstudien nimmt die NMR-Spektroskopie eine unersetzliche Rolle ein, da sie die einzige Methode darstellt, die es ermöglicht, sowohl die Struktur eines Proteins als auch dessen dynamische Prozesse auf atomarer Ebene unter Natur-ähnlichen Bedingungen zu untersuchen. Protein-NMR-Spektroskopie durchlief in den vergangenen Jahrzehnten eminente Entwicklungen, die oftmals erst durch den Entwurf neuer Isotopen-Markierungsstrategien ermöglicht wurden.

Die selektive Einbringung CD_2H-markierter Methylgruppen in perdeuterierte Proteine erwies sich als wertvolle Möglichkeit für die Detektion dynamischer Daten. Darüber hinaus weisen hydrophobe Proteinbereiche häufig eine hohe Konzentration an Methylgruppen auf, weshalb sich diese hervorragend als Sonden für Untersuchungen von Protein-Ligand-Wechselwirkungen eignen.

Eine bewährte Methode für selektive Isotopenmarkierung von Proteinen ist die heterologe Überexpression des gewünschten Proteins in Anwesenheit einer entsprechend markierten Aminosäure-Vorstufe in gentechnisch manipulierten Bakterienstämmen. Das Ziel dieser Masterarbeit war die Entwicklung eines Synthesewegs zur Herstellung von CD_2H-Methylgruppen-markierten Leucin- bzw. Isoleucin-Vorläufermolekülen ausgehend von preiswerten Ausgangsmaterialien.

Als Leucin-Vorstufe wurde α-Ketoisocaproate ausgewählt, während für Isoleucin α-Keto-β-methylvalerat als Vorstufe bestimmt wurde. Der erste Schritt des Synthesewegs, der für beide Vorstufenmoleküle gilt, stellt die Einbringung einer CD_2-Methylengruppe mittels der Wittig-Reaktion dar. Dieser erste Reaktionsschritt erwies sich als derart große Herausforderung, dass der Gegenstand dieser Arbeit auf das Ermitteln der geeigneten Reaktionsbedingungen der Wittig-Reaktion beschränkt wurde. In 1-(Tetrahydropyran-2-yloxy)-2-propanon, eine Vorläuferverbindung von α-Ketoisocaproate, konnte eine CD_2-Methylengruppe erfolgreich eingebracht werden.

6.3 List of abbreviations

Å	Ångström
CRINEPT	Cross-correlated relaxation-enhanced polarization transfer
CRIPT	Cross-relaxation induced polarization transfer
d	Doublet
D_2O	Deuterium oxide
DCM	Dichlormethane
DMF	Dimethylformamide
dt	Doublet of triplets
E.coli	*Escherichia coli*
HCl	Hydrogen chloride
HMQC	Heteronuclear multiple-quantum correlation spectroscopy
HSQC	Heteronuclear single-quantum correlation spectroscopy
HZQC	Heteronuclear zero-quantum coherence
INEPT	Insensitive nuclei enhanced by polarization transfer
LDA	Lithium diisopropylamide
m	Multiplet
$MgSO_4$	Magnesium sulphate
NaHMDS	Sodium bis(trimethylsilyl)amide
n-BuLi	*n*-Butyllithium
NMR	Nuclear magnetic resonance
NOESY	^{15}N-edited Nuclear Overhauser Effect Spectroscopy
ppm	Parts per million
rt	Room temperature
s	Singlet
t	Triplet
t-BuOK	Potassium *tert*-butoxide
THF	Tetrahydrofuran
TLC	Thin-layer chromatography
TROSY	Transverse relaxation optimized spectroscopy
TOCSY	Total Correlation Spectroscopy
δ	Chemical shift

6.4 List of references

1. Becker, E. D., A Brief History of Nuclear Magnetic Resonance. *Analytical Chemistry* **1993,** *65* (6), 295A-302A.
2. Purcell, E. M.; Torrey, H. C.; Pound, R. V., Resonance Absorption by Nuclear Magnetic Moments in a Solid. *Physical Review* **1946,** *69* (1-2), 37-38.
3. Bloch, F.; Hansen, W. W.; Packard, M., Nuclear Induction. *Physical Review* **1946,** *69* (3-4), 127-127.
4. Kerfah, R.; Plevin, M. J.; Sounier, R.; Gans, P.; Boisbouvier, J., Methyl-specific isotopic labeling: a molecular tool box for solution NMR studies of large proteins. *Current Opinion in Structural Biology* **2015,** *32*, 113-122.
5. Kay, L. E., New Views of Functionally Dynamic Proteins by Solution NMR Spectroscopy. *Journal of Molecular Biology* **2016,** *428* (2, Part A), 323-331.
6. Emsley, J. W.; Feeney, J., Forty years of Progress in Nuclear Magnetic Resonance Spectroscopy. *Progress in Nuclear Magnetic Resonance Spectroscopy* **2007,** *50* (4), 179-198.
7. Gong, Z.; Schwieters, C. D.; Tang, C., Conjoined Use of EM and NMR in RNA Structure Refinement. *PLoS ONE* **2015,** *10* (3), e0120445.
8. Palmer, A. G.; Patel, D. J., Kurt Wüthrich and NMR of Biological Macromolecules. *Structure* **2002,** *10* (12), 1603-1604.
9. Kempf, J. G.; Loria, J. P., Protein dynamics from solution NMR: theory and applications. *Cell Biochem Biophys* **2003,** *37* (3), 187-211.
10. Wand, A. J., Dynamic activation of protein function: A view emerging from NMR spectroscopy. *Nat Struct Mol Biol* **2001,** *8* (11), 926-931.
11. Ballaschk, M. Quo vadis NMR? – Ein Gespräch mit Kurt Wüthrich. http://www.lindau-nobel.org/quo-vadis-nmr-ein-gesprach-mit-kurt-wuthrich/ (accessed 08.04.2016).
12. Ruschak, A. M.; Kay, L. E., Methyl groups as probes of supra-molecular structure, dynamics and function. *J Biomol NMR* **2010,** *46* (1), 75-87.
13. Gardner, K. H.; Kay, L. E., The use of 2H, 13C, 15N multidimensional NMR to study the structure and dynamics of proteins. *Annu Rev Biophys Biomol Struct* **1998,** *27*, 357-406.
14. Wijmenga, S. S.; Hallenga, K.; Hilbers, C. W., A three-dimensional heteronuclear multiple-quantum coherence homonuclear hartmann-hahn experiment. *Journal of Magnetic Resonance (1969)* **1989,** *84* (3), 634-642.
15. Marion, D.; Driscoll, P. C.; Kay, L. E.; Wingfield, P. T.; Bax, A.; Gronenborn, A. M.; Clore, G. M., Overcoming the overlap problem in the assignment of 1H NMR spectra of larger proteins by use of three-dimensional heteronuclear 1H-15N Hartmann-Hahn-multiple quantum coherence and nuclear Overhauser-multiple quantum coherence spectroscopy: application to interleukin 1 beta. *Biochemistry* **1989,** *28* (15), 6150-6.
16. Tugarinov, V.; Kay, L. E., An Isotope Labeling Strategy for Methyl TROSY Spectroscopy. *Journal of Biomolecular NMR* **2004,** *28* (2), 165-172.
17. Tugarinov, V.; Hwang, P. M.; Ollerenshaw, J. E.; Kay, L. E., Cross-Correlated Relaxation Enhanced 1H−13C NMR Spectroscopy of Methyl Groups in Very High Molecular Weight Proteins and Protein Complexes. *Journal of the American Chemical Society* **2003,** *125* (34), 10420-10428.
18. Takeda, M.; Kainosho, M., Isotope Labelling. In *Protein NMR Spectroscopy: Practical Techniques and Applications*, John Wiley & Sons, Ltd: **2011**, pp 23-53.
19. Ohki, S.-y.; Kainosho, M., Stable isotope labeling methods for protein NMR spectroscopy. *Progress in Nuclear Magnetic Resonance Spectroscopy* **2008,** *53* (4), 208-226.
20. Farmer, B., II; Venters, R., NMR of Perdeuterated Large Proteins. In *Modern Techniques in Protein NMR*, Krishna, N. R.; Berliner, L., Eds. Springer US: **2002**; Chapter 3, pp 75-120.
21. Chizhik, V. I.; Chernyshev, Y. S.; Donets, A. V.; Frolov, V.; Komolkin, A.; Shelyapina, M. G., *Magnetic Resonance and Its Applications*. Springer International Publishing: **2014**.
22. Tugarinov, V.; Kay, L. E., Methyl Groups as Probes of Structure and Dynamics in NMR Studies of High-Molecular-Weight Proteins. *ChemBioChem* **2005,** *6* (9), 1567-1577.
23. Markus, M. A.; Dayie, K. T.; Matsudaira, P.; Wagner, G., Effect of Deuteration on the Amide Proton Relaxation Rates in Proteins. Heteronuclear NMR Experiments on Villin 14T. *Journal of Magnetic Resonance, Series B* **1994,** *105* (2), 192-195.

24. Hoogstraten, C. G.; Johnson, J. E., Metabolic labeling: Taking advantage of bacterial pathways to prepare spectroscopically useful isotope patterns in proteins and nucleic acids. *Concepts in Magnetic Resonance Part A* **2008,** *32A* (1), 34-55.
25. Nilsson, B. L.; Soellner, M. B.; Raines, R. T., Chemical Synthesis of Proteins. *Annual review of biophysics and biomolecular structure* **2005,** *34*, 91-118.
26. Saxena, K.; Dutta, A.; Klein-Seetharaman, J.; Schwalbe, H., Isotope Labeling in Insect Cells. *Methods in molecular biology (Clifton, N.J.)* **2012,** *831*, 37-54.
27. Sørensen, H. P.; Mortensen, K. K., Advanced genetic strategies for recombinant protein expression in Escherichia coli. *Journal of Biotechnology* **2005,** *115* (2), 113-128.
28. Baneyx, F., Recombinant protein expression in Escherichia coli. *Current Opinion in Biotechnology* **1999,** *10* (5), 411-421.
29. Makrides, S. C., Strategies for achieving high-level expression of genes in Escherichia coli. *Microbiological reviews* **1996,** *60* (3), 512-38.
30. Lodish, H.; Berk, A.; Zipursky, S. L., *Molecular Cell Biology*. W H Freeman & Co: New York, **2000**.
31. Driscoll, P. C., Macromolecular Complexes. In *Protein NMR Spectroscopy: Practical Techniques and Applications*, John Wiley & Sons, Ltd: **2011**, pp 269-317.
32. Miyanoiri, Y.; Takeda, M.; Okuma, K.; Ono, A.; Terauchi, T.; Kainosho, M., Differential isotope-labeling for Leu and Val residues in a protein by E. coli cellular expression using stereo-specifically methyl labeled amino acids. *Journal of Biomolecular NMR* **2013,** *57* (3), 237-249.
33. Atreya, H. S., *Isotope labeling in Biomolecular NMR*. Springer Netherlands: **2012**.
34. Lian, L.-Y.; Middleton, D. A., *Labelling approaches for protein structural studies by solution-state and solid-state NMR*. **2001**; Vol. 39, p 171-190.
35. Su, X. C.; Loh, C. T.; Qi, R.; Otting, G., Suppression of isotope scrambling in cell-free protein synthesis by broadband inhibition of PLP enymes for selective 15N-labelling and production of perdeuterated proteins in H2O. *J Biomol NMR* **2011,** *50* (1), 35-42.
36. Takeuchi, K.; Sun, Z.-Y. J.; Wagner, G., Alternate ^{13}C Labeling for Complete Mainchain Resonance Assignments using Cα Direct-Detection with Applicability Toward Fast Relaxing Protein Systems. *Journal of the American Chemical Society* **2008,** *130* (51), 17210-17211.
37. KEGG Valine, leucine and isoleucine biosynthesis. http://www.genome.jp/kegg-bin/show_pathway?map=map00290&show_description=show (accessed 19.04.2016).
38. Ayala, I.; Hamelin, O.; Amero, C.; Pessey, O.; Plevin, M. J.; Gans, P.; Boisbouvier, J., An optimized isotopic labelling strategy of isoleucine-[gamma]2 methyl groups for solution NMR studies of high molecular weight proteins. *Chemical Communications* **2012,** *48* (10), 1434-1436.
39. Lichtenecker, R., unpublished data.
40. Lichtenecker, R. J.; Coudevylle, N.; Konrat, R.; Schmid, W., Selective isotope labelling of leucine residues by using alpha-ketoacid precursor compounds. *Chembiochem* **2013,** *14* (7), 818-21.
41. Lichtenecker, R. J.; Weinhaupl, K.; Reuther, L.; Schorghuber, J.; Schmid, W.; Konrat, R., Independent valine and leucine isotope labeling in Escherichia coli protein overexpression systems. *J Biomol NMR* **2013,** *57* (3), 205-9.
42. Kempf, J.; Loria, J. P., Protein dynamics from solution NMR. *Cell Biochemistry and Biophysics* **2002,** *37* (3), 187-211.
43. Ollerenshaw, J. E.; Tugarinov, V.; Kay, L. E., Methyl TROSY: explanation and experimental verification. *Magnetic Resonance in Chemistry* **2003,** *41* (10), 843-852.
44. Wiesner, S.; Sprangers, R., Methyl groups as NMR probes for biomolecular interactions. *Current Opinion in Structural Biology* **2015,** *35*, 60-67.
45. Pervushin, K.; Riek, R.; Wider, G.; Wüthrich, K., Attenuated T2 relaxation by mutual cancellation of dipole–dipole coupling and chemical shift anisotropy indicates an avenue to NMR structures of very large biological macromolecules in solution. *Proceedings of the National Academy of Sciences* **1997,** *94* (23), 12366-12371.
46. Tugarinov, V.; Kay, L. E., Separating Degenerate 1H Transitions in Methyl Group Probes for Single-Quantum 1H-CPMG Relaxation Dispersion NMR Spectroscopy. *Journal of the American Chemical Society* **2007,** *129* (30), 9514-9521.

47. Ollerenshaw, J.; Tugarinov, V.; Skrynnikov, N.; Kay, L., Comparison of 13CH3, 13CH2D, and 13CHD2 methyl labeling strategies in proteins. *Journal of Biomolecular NMR* **2005,** *33* (1), 25-41.
48. Tugarinov, V.; Sprangers, R.; Kay, L. E., Line Narrowing in Methyl-TROSY Using Zero-Quantum 1H-13C NMR Spectroscopy. *Journal of the American Chemical Society* **2004,** *126* (15), 4921-4925.
49. Liao, X.; Tugarinov, V., Selective detection of 13CHD2 signals from a mixture of 13CH3/13CH2D/13CHD2 methyl isotopomers in proteins. *Journal of Magnetic Resonance* **2011,** *209* (1), 101-107.
50. Weininger, U.; Blissing, A. T.; Hennig, J.; Ahlner, A.; Liu, Z.; Vogel, H. J.; Akke, M.; Lundstrom, P., Protein conformational exchange measured by 1H R1rho relaxation dispersion of methyl groups. *J Biomol NMR* **2013,** *57* (1), 47-55.
51. Ishima, R.; Louis, J. M.; Torchia, D. A., Transverse 13C Relaxation of CHD2 Methyl Isotopmers To Detect Slow Conformational Changes of Protein Side Chains. *Journal of the American Chemical Society* **1999,** *121* (49), 11589-11590.
52. Otten, R.; Villali, J.; Kern, D.; Mulder, F. A. A., Probing Microsecond Time Scale Dynamics in Proteins by Methyl (1)H Carr−Purcell−Meiboom−Gill Relaxation Dispersion NMR Measurements. Application to Activation of the Signaling Protein NtrC(r). *Journal of the American Chemical Society* **2010,** *132* (47), 17004-17014.
53. Bain, A. D., Dynamic NMR. In *Modern NMR Techniques for Synthetic Chemistry*, CRC Press: **2014**, pp 15-62.
54. Hahn, E. L., Spin Echoes. *Physical Review* **1950,** *80* (4), 580-594.
55. Carr, H. Y.; Purcell, E. M., Effects of Diffusion on Free Precession in Nuclear Magnetic Resonance Experiments. *Physical Review* **1954,** *94* (3), 630-638.
56. Meiboom, S.; Gill, D., Modified Spin-Echo Method for Measuring Nuclear Relaxation Times. *Review of Scientific Instruments* **1958,** *29* (8), 688-691.
57. Ishima, R.; Louis, J. M.; Torchia, D. A., Optimized labeling of 13CHD2 methyl isotopomers in perdeuterated proteins: potential advantages for 13C relaxation studies of methyl dynamics of larger proteins. *J Biomol NMR* **2001,** *21* (2), 167-71.
58. Tugarinov, V.; Kanelis, V.; Kay, L. E., Isotope labeling strategies for the study of high-molecular-weight proteins by solution NMR spectroscopy. *Nat. Protocols* **2006,** *1* (2), 749-754.
59. Tugarinov, V.; Ollerenshaw, J. E.; Kay, L. E., Probing Side-Chain Dynamics in High Molecular Weight Proteins by Deuterium NMR Spin Relaxation: An Application to an 82-kDa Enzyme. *Journal of the American Chemical Society* **2005,** *127* (22), 8214-8225.
60. Tugarinov, V.; Kay, L. E., Quantitative 13C and 2H NMR Relaxation Studies of the 723-Residue Enzyme Malate Synthase G Reveal a Dynamic Binding Interface. *Biochemistry* **2005,** *44* (49), 15970-15977.
61. Baldwin, A. J.; Religa, T. L.; Hansen, D. F.; Bouvignies, G.; Kay, L. E., 13CHD2 Methyl Group Probes of Millisecond Time Scale Exchange in Proteins by 1H Relaxation Dispersion: An Application to Proteasome Gating Residue Dynamics. *Journal of the American Chemical Society* **2010,** *132* (32), 10992-10995.
62. Goto, N. K.; Gardner, K. H.; Mueller, G. A.; Willis, R. C.; Kay, L. E., A robust and cost-effective method for the production of Val, Leu, Ile (δ1) methyl-protonated 15N-, 13C-, 2H-labeled proteins. *Journal of Biomolecular NMR 13* (4), 369-374.
63. Gardner, K. H.; Kay, L. E., Production and Incorporation of 15N, 13C, 2H (1H-δ1 Methyl) Isoleucine into Proteins for Multidimensional NMR Studies. *Journal of the American Chemical Society* **1997,** *119* (32), 7599-7600.
64. Lyudmila, A. Y., The Wittig Reaction. *Russian Chemical Reviews* **1961,** *30* (7), 347-361.
65. Staudinger, H.; Meyer, J., Über neue organische Phosphorverbindungen III. Phosphinmethylenderivate und Phosphinimine. *Helvetica Chimica Acta* **1919,** *2* (1), 635-646.
66. Wittig, G. Nobel Lecture: From Diyls to Ylides to My Idyll. http://www.nobelprize.org/nobel_prizes/chemistry/laureates/1979/wittig-lecture.html (accessed 03.04.2016).
67. Wittig, G.; Geissler, G., Zur Reaktionsweise des Pentaphenyl-phosphors und einiger Derivate. *Justus Liebigs Annalen der Chemie* **1953,** *580* (1), 44-57.

68. Byrne, P. A.; Gilheany, D. G., The modern interpretation of the Wittig reaction mechanism. *Chemical Society Reviews* **2013,** *42* (16), 6670-6696.
69. Edmonds, M.; Abell, A., The Wittig Reaction. In *Modern Carbonyl Olefination*, Wiley-VCH Verlag GmbH & Co. KGaA: **2004**, pp 1-17.
70. Nelson, W. M., *Green Solvents for Chemistry: Perspectives and Practice* Oxford University Press: New York, **2003**.
71. Makino, K.; Goto, T.; Hiroki, Y.; Hamada, Y., Direct anti-selective asymmetric hydrogenation of α-amino-β-keto esters through dynamic kinetic resolution using Ru-axially chiral phosphine catalysts—stereoselective synthesis of anti-β-hydroxy-α-amino acids. *Tetrahedron: Asymmetry* **2008,** *19* (24), 2816-2828.
72. Trost, B. M.; Fettes, A.; Shireman, B. T., Direct Catalytic Asymmetric Aldol Additions of Methyl Ynones. Spontaneous Reversal in the Sense of Enantioinduction. *Journal of the American Chemical Society* **2004,** *126* (9), 2660-2661.
73. Arican, D.; Brückner, R., Syntheses of 3,4-Benzotropolones by Ring-Closing Metatheses. *Organic Letters* **2013,** *15* (11), 2582-2585.
74. Hoyer, S.; Laszlo, P.; Orlović, M.; Polla, E., Catalysis by Acidic Clay of the Protective Tetrahydropyranylation of Alcohols and Phenols. *Synthesis* **1986,** *1986* (08), 655-657.
75. Deng, Z.; Wei, J.; Liao, L.; Huang, H.; Zhao, X., Organoselenium-Catalyzed, Hydroxy-Controlled Regio- and Stereoselective Amination of Terminal Alkenes: Efficient Synthesis of 3-Amino Allylic Alcohols. *Organic Letters* **2015,** *17* (8), 1834-1837.
76. Yamamoto, M.; Oshima, K.; Matsubara, S., Preparation of Deuterium Labelled Organophosphonium Salts (Wittig Salts) under Hydrothermal Condition Catalyzed by Molecular Sieves. *Chemistry Letters* **2004,** *33* (7), 846-847.

6.5 Reference list for figures and tabels

Atreya, H. S., Isotope labeling in Biomolecular NMR. Springer Netherlands: **2012**.

Byrne, P. A.; Gilheany, D. G., The modern interpretation of the Wittig reaction mechanism. *Chemical Society Reviews* **2013,** *42* (16), 6670-6696.

Lian, L.-Y.; Middleton, D. A., Labelling approaches for protein structural studies by solution-state and solid-state NMR. **2001**; Vol. 39, p 171-190.

Lichtenecker, R. J.; Weinhaupl, K.; Reuther, L.; Schorghuber, J.; Schmid, W.; Konrat, R., Independent valine and leucine isotope labeling in Escherichia coli protein overexpression systems. *J Biomol NMR* **2013,** *57* (3), 205-9.

Ollerenshaw, J.; Tugarinov, V.; Skrynnikov, N.; Kay, L., Comparison of 13CH3, 13CH2D, and 13CHD2 methyl labeling strategies in proteins. *Journal of Biomolecular NMR* **2005,** *33* (1), 25-41.

6.6 Spectra

Ethyl 4-oxo-2,2-(propylenedioxo)-pentanoate (1)(^{1}H NMR, 400.3 MHz, $CDCl_3$)

:

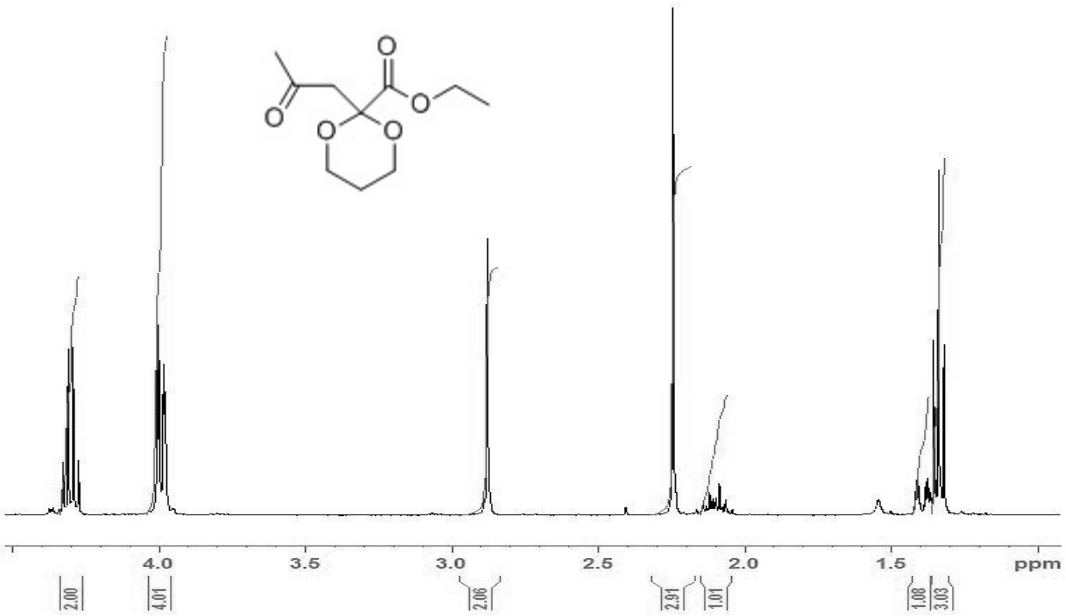

Ethyl 4-oxo-2,2-(propylenedioxo)-pentanoate (1) (^{13}C, 100.6 MHz, CDCl3)

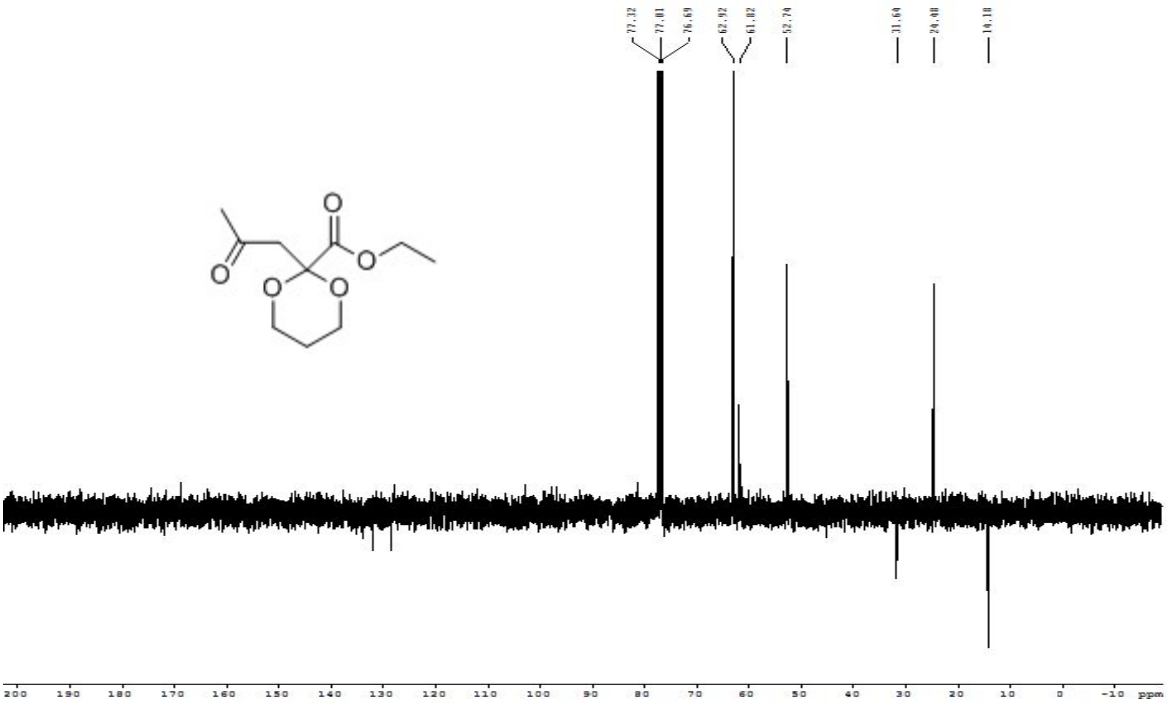

Methyl 2,2-dimethoxy-4-oxopentanoate (2) (^{1}H NMR (400.3 MHz, $CDCl_3$)

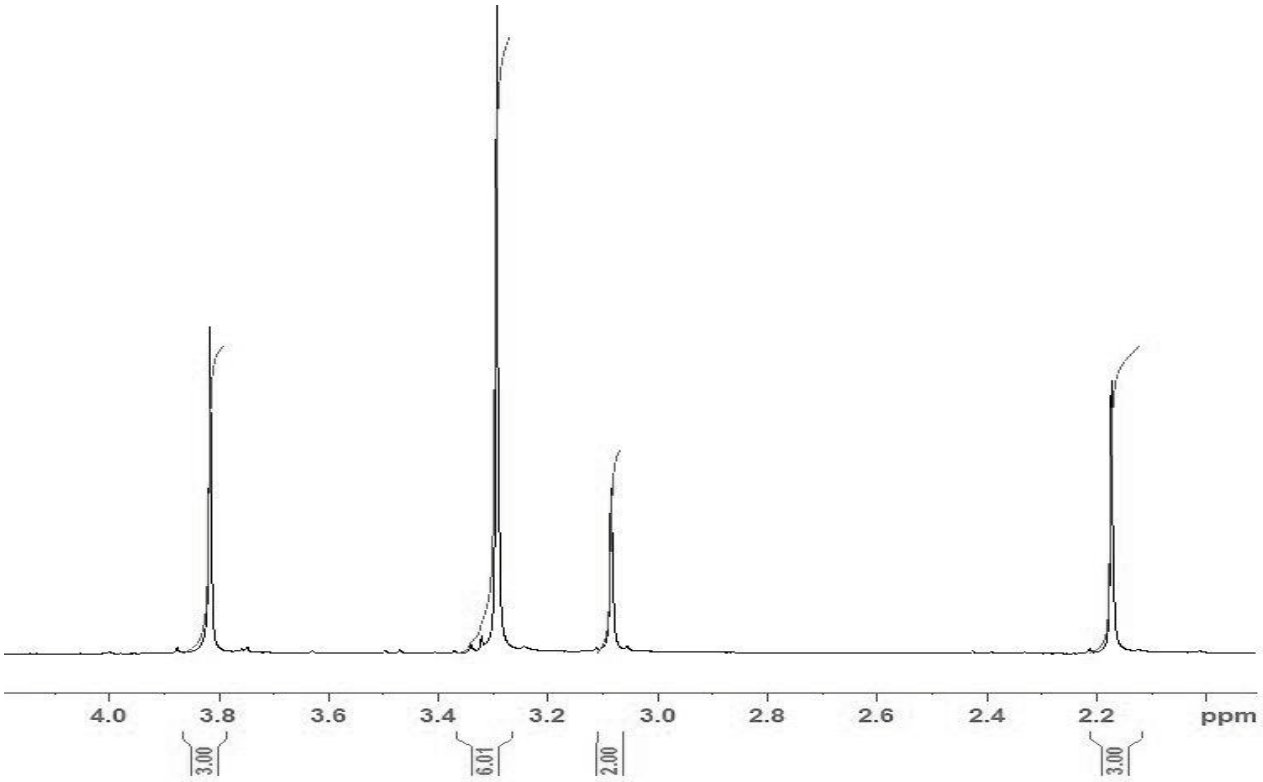

Methyl 2,2-dimethoxy-4-oxobutanoate (5) (^{1}H NMR (400.3 MHz, $CDCl_3$)

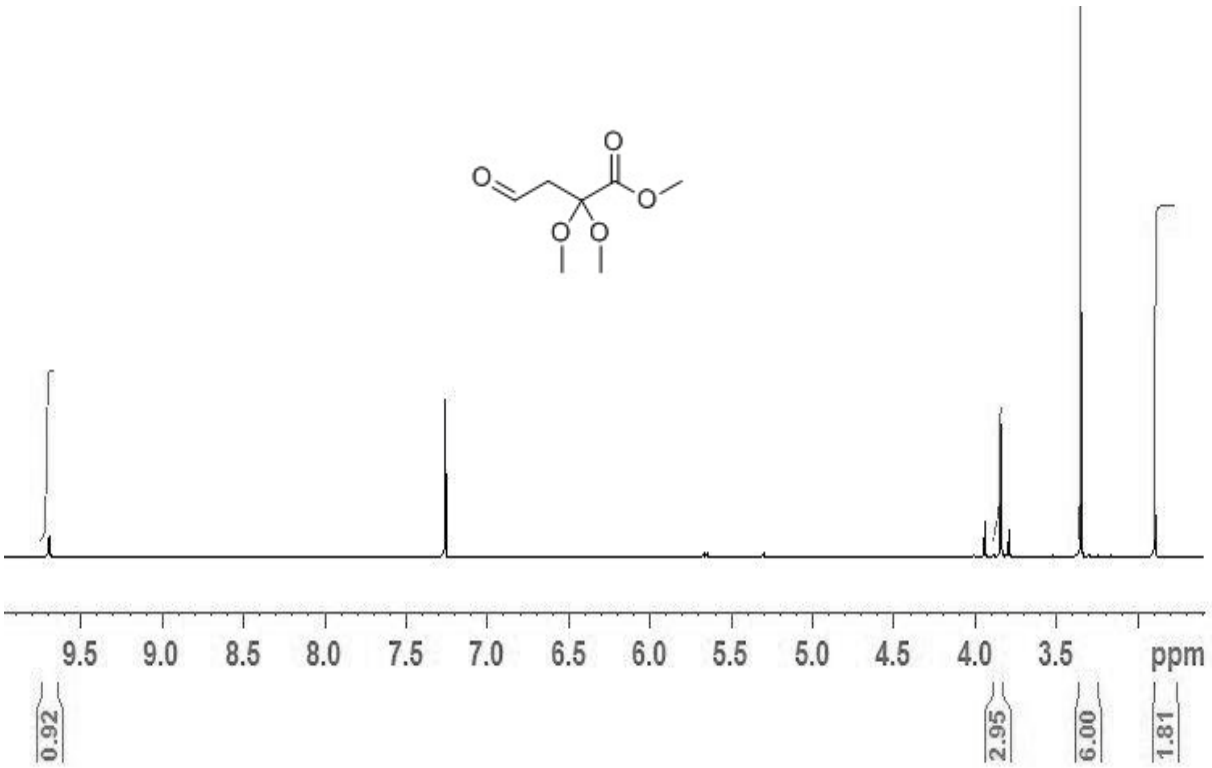

Methyl 2,2-dimethoxy-4-oxobutanoate (5) (^{13}C (100.6 MHz, CDCl3)

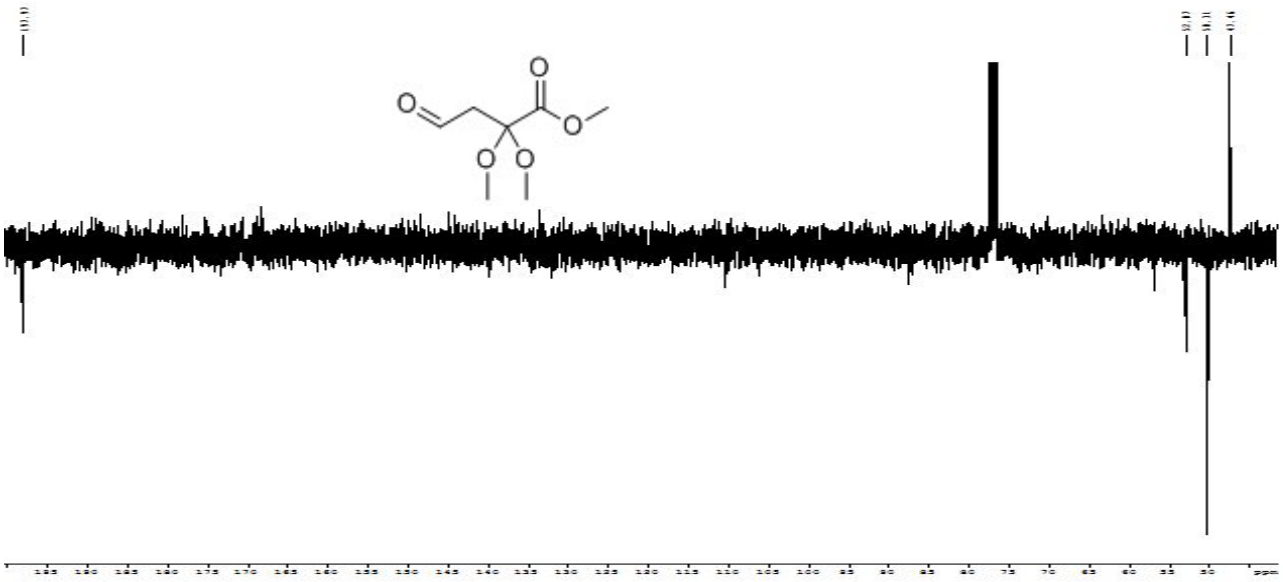

1-(tetrahydropyran-2-yloxy)-2-propanone (6) (^{1}H NMR (400.3 MHz, $CDCl_3$)

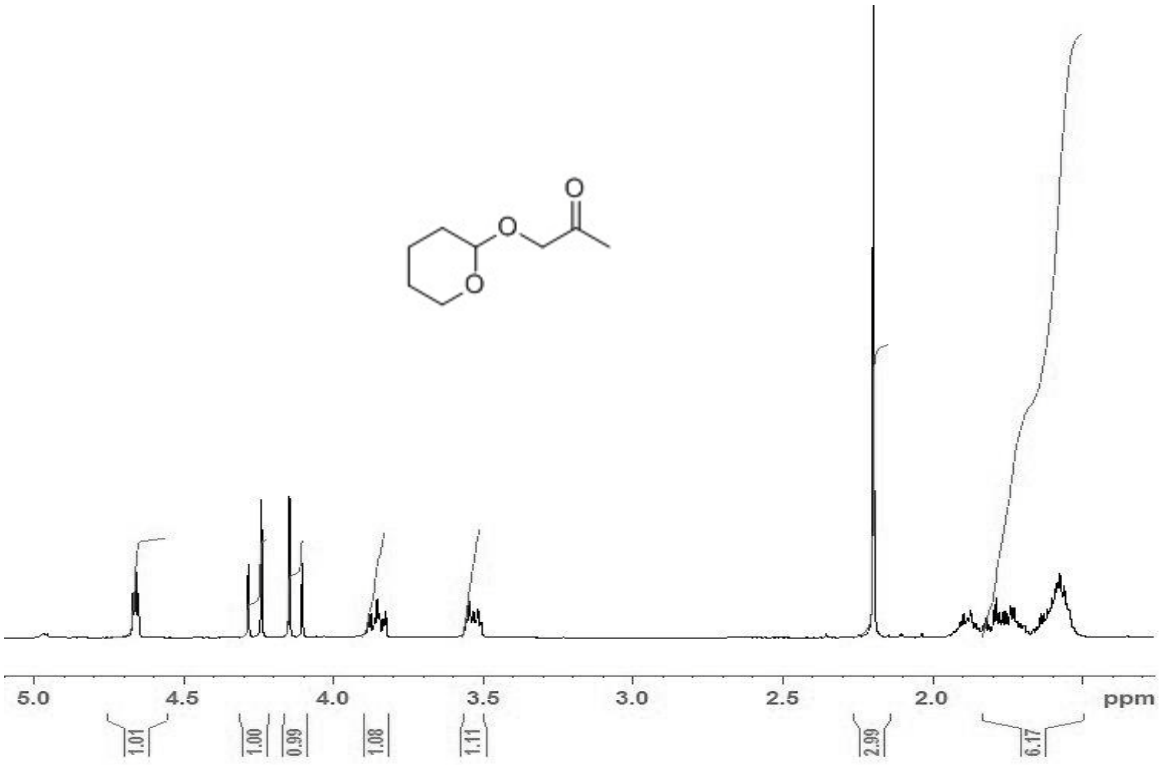

1-(tetrahydropyran-2-yloxy)-2-propanone (6) (^{13}C (100.6 MHz, CDCl3)

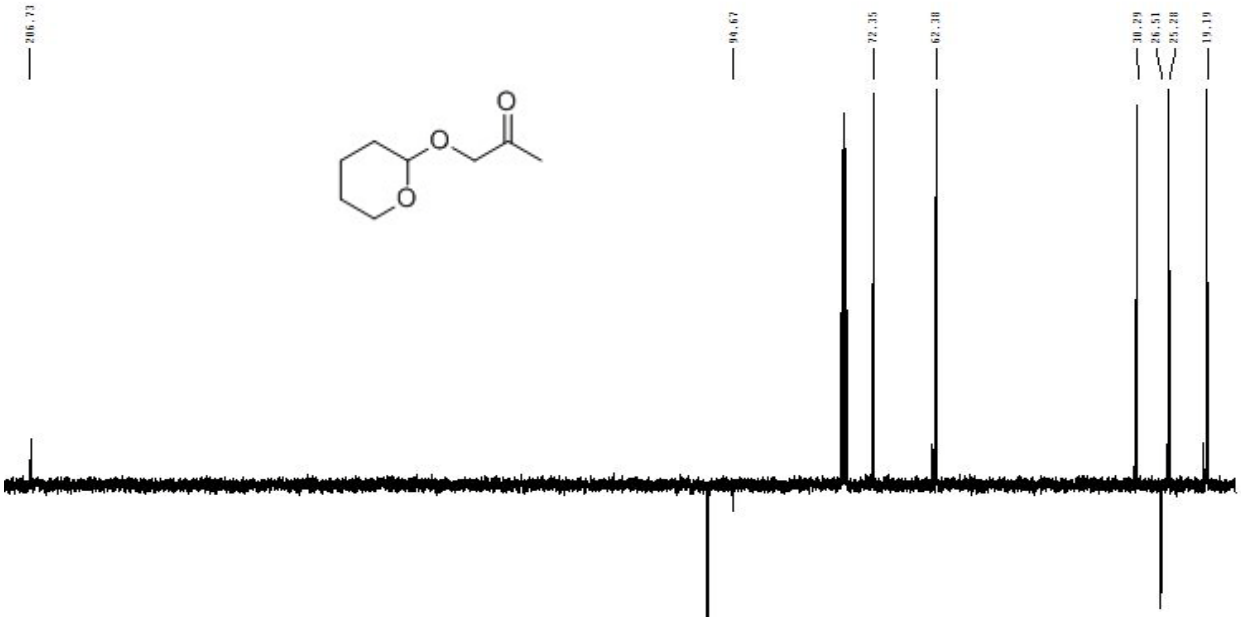

Ethyl 1,3-dioxane-2-carboxylate (13) (^{1}H NMR (400.3 MHz, $CDCl_3$)

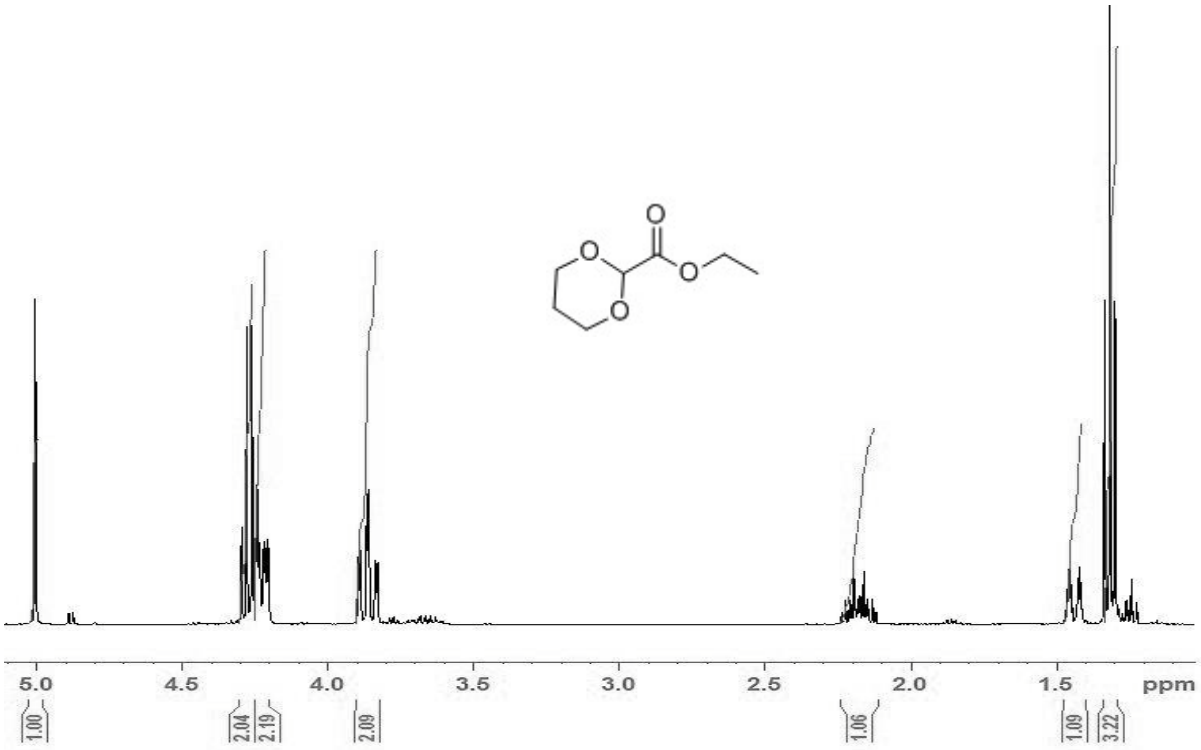

Ethyl 1,3-dioxane-2-carboxylate (13) (^{13}C (100.6 MHz, $CDCl_3$)

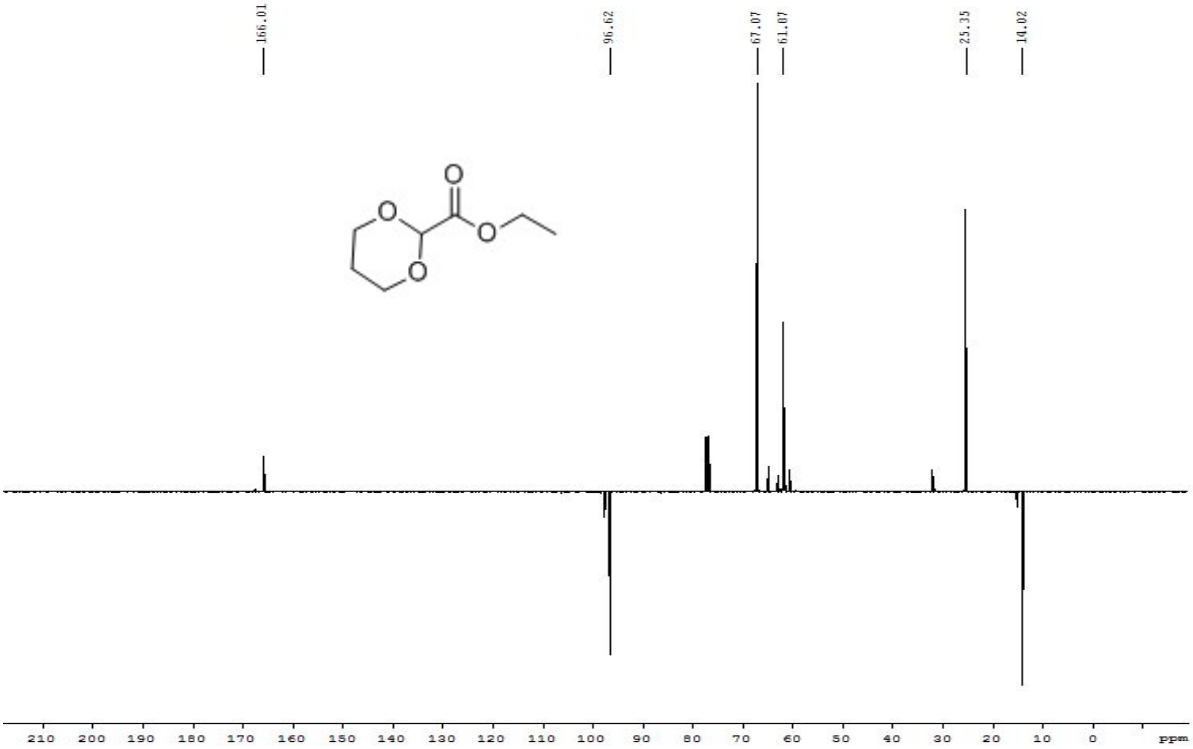

Ethyl 4-methylidene-2,2-(propylenedioxo)-pentanoate (14) (^{1}H NMR (400.3 MHz, $CDCl_3$)

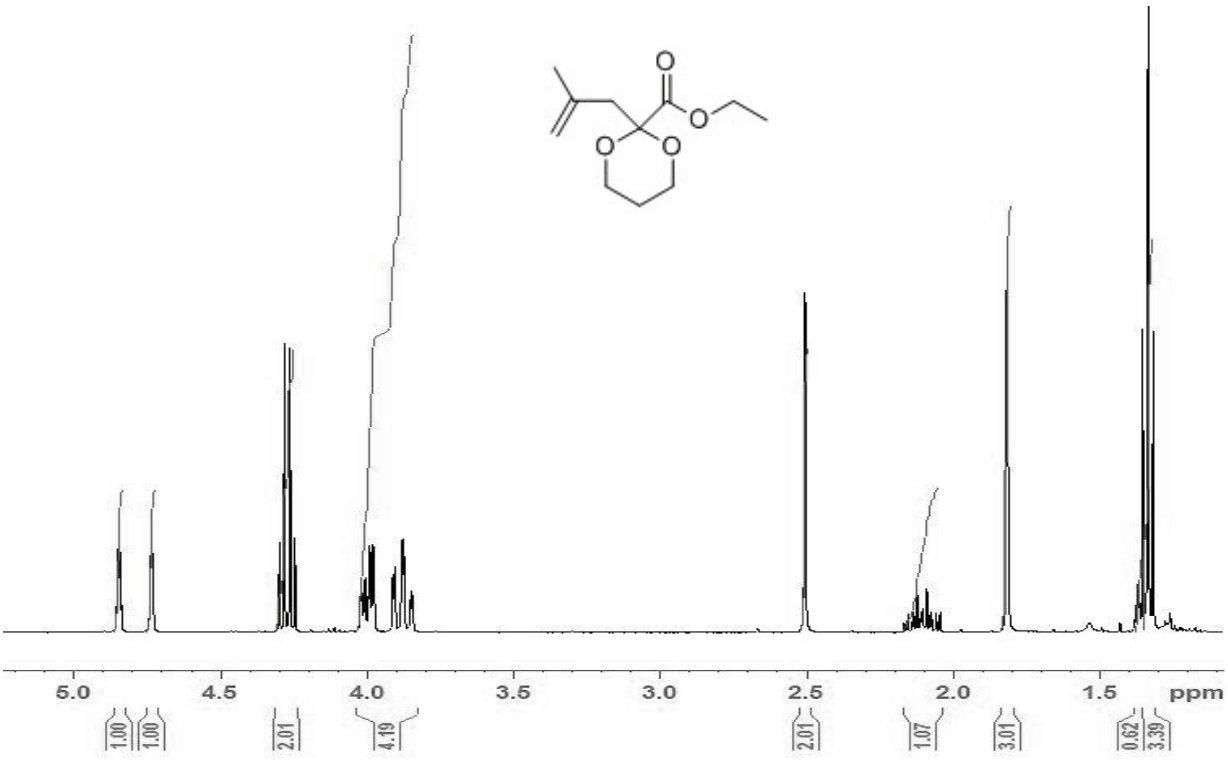

Ethyl 4-methylidene-2,2-(propylenedioxo)-pentanoate (14) (^{13}C (100.6 MHz, CDCl3)

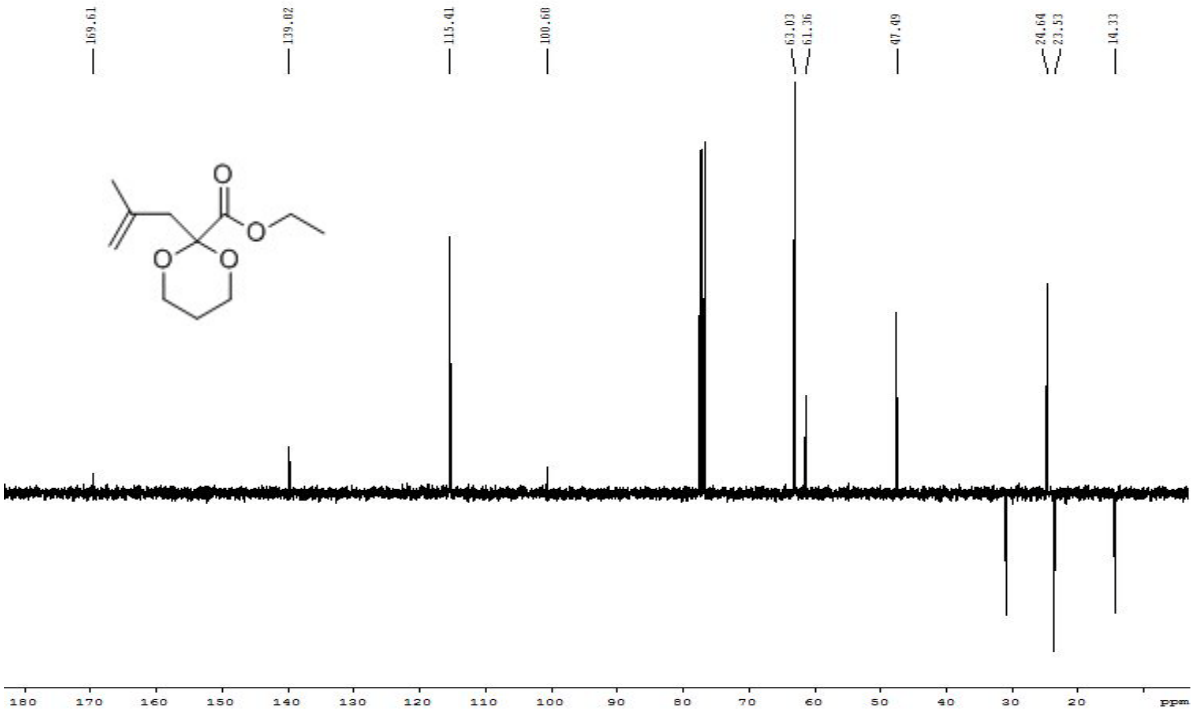

Methyl 2,2-dimethoxyacetate (15) (^{1}H NMR (400.3 MHz, $CDCl_3$)

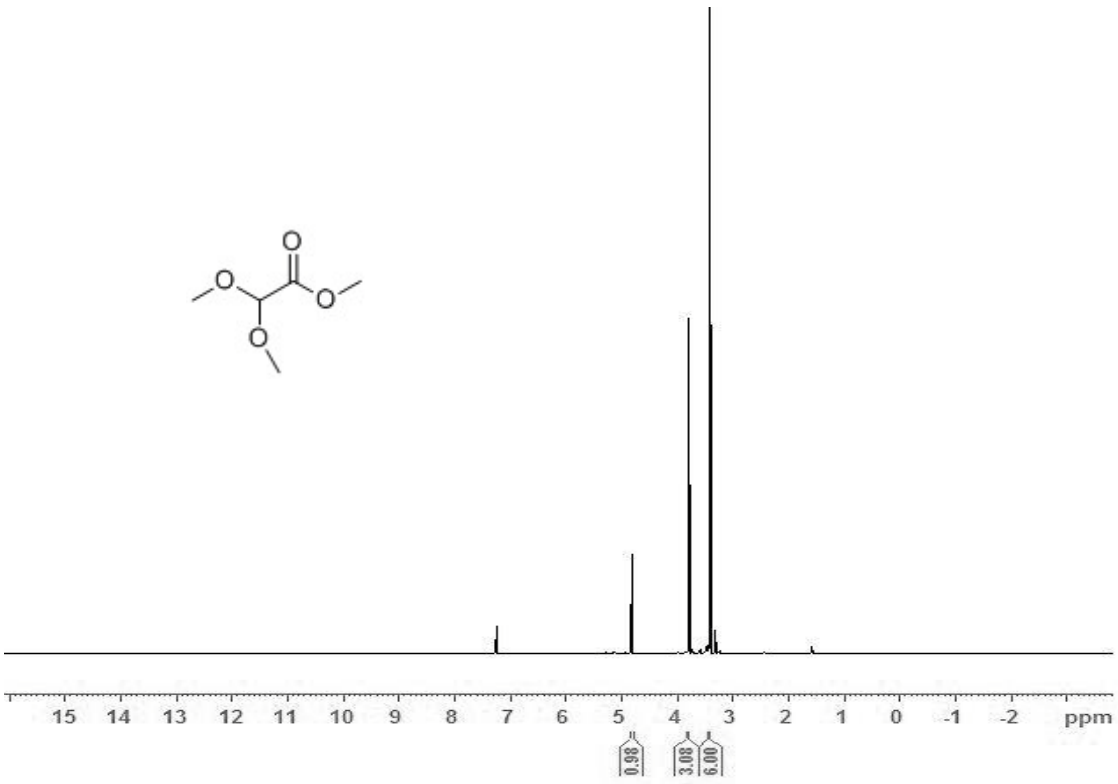

Methyl 2,2-dimethoxy-4-methylidene-pentanoate (16) (^{1}H NMR (400.3 MHz, $CDCl_3$)

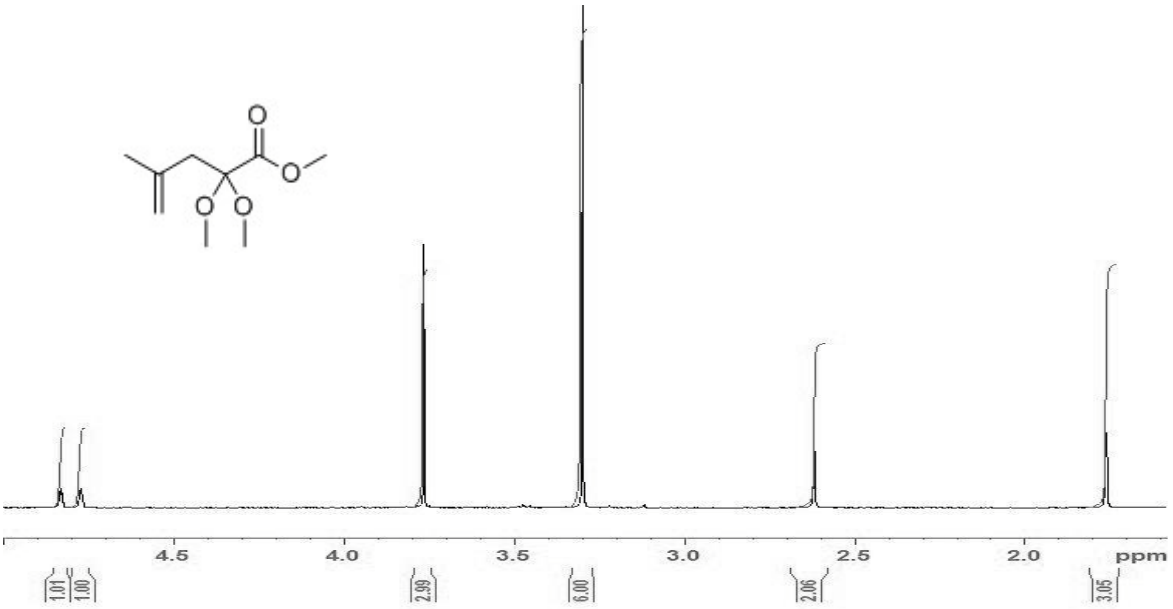

Methyl 2,2-dimethoxy-4-methylidene-pentanoate (16) (^{13}C (100.6 MHz, CDCl3)

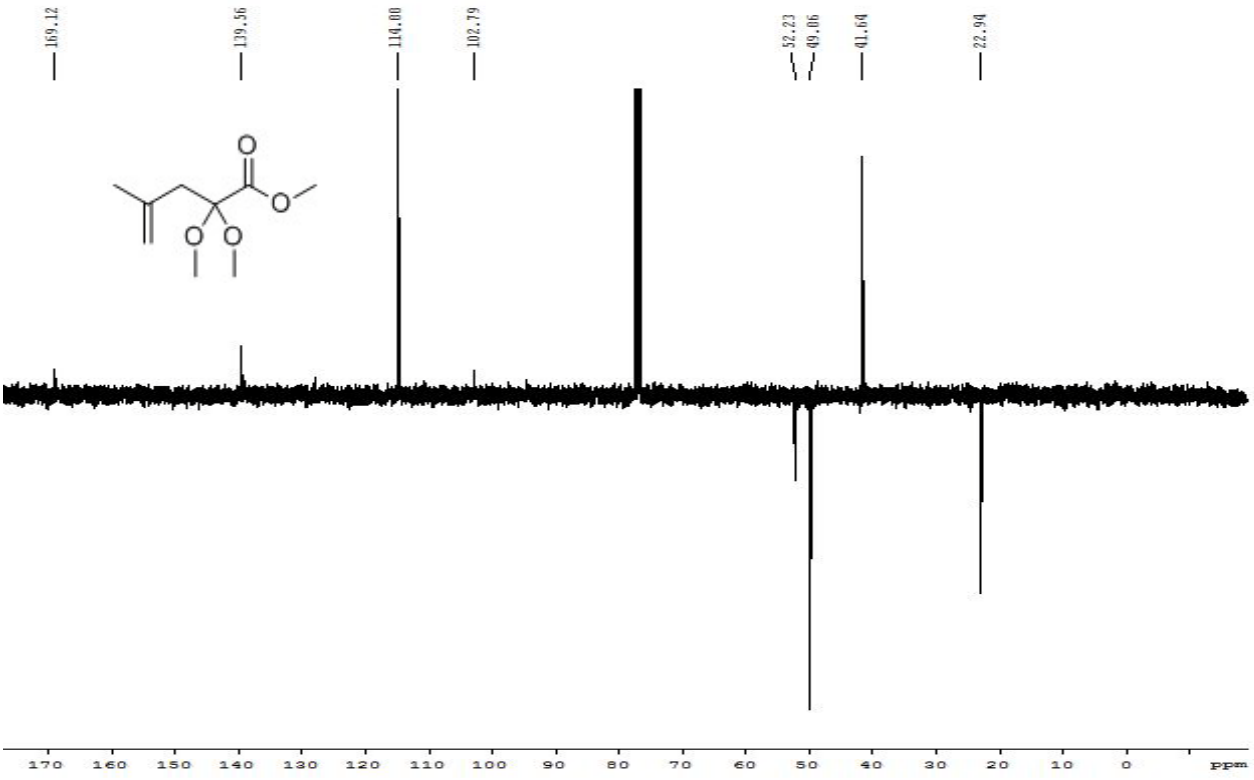

Methyl 2,2-dimethoxy-4-methylene-butanoate (17) (^{1}H NMR (400.3 MHz, $CDCl_3$)

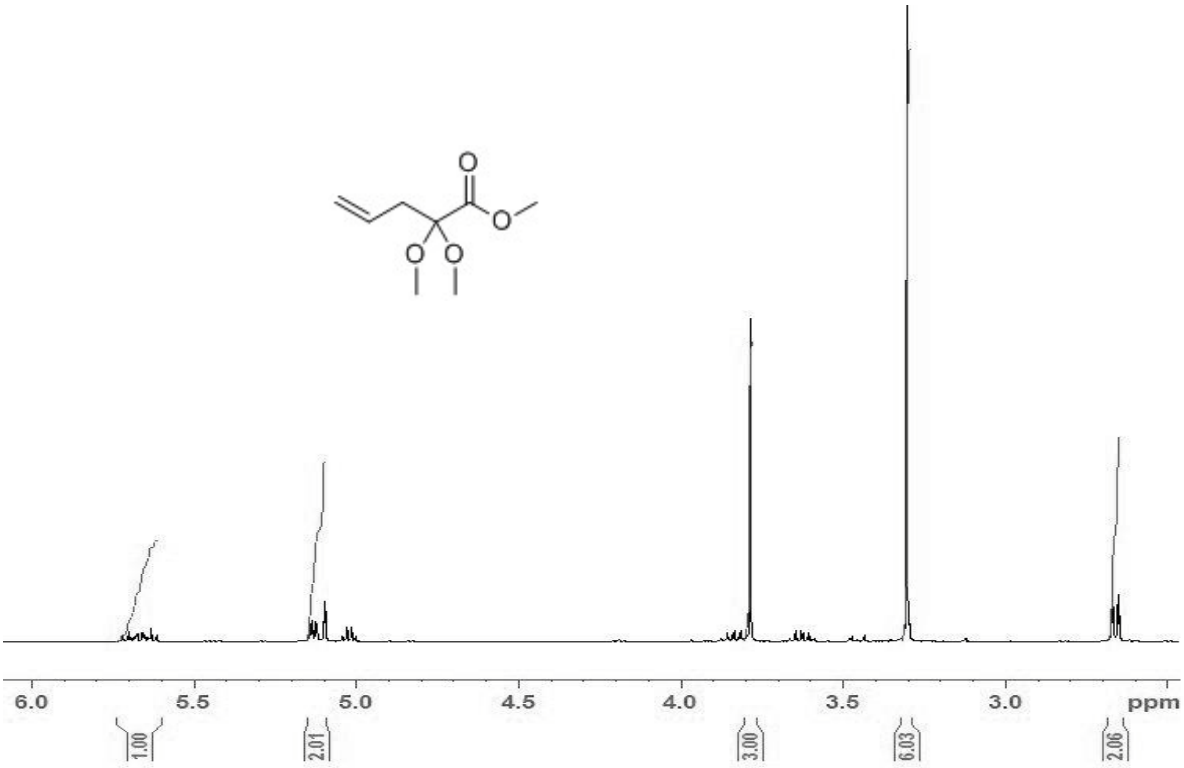

Methyltriphenylphosphonium iodide (18) (^{1}H NMR (400.3 MHz, $CDCl_3$):

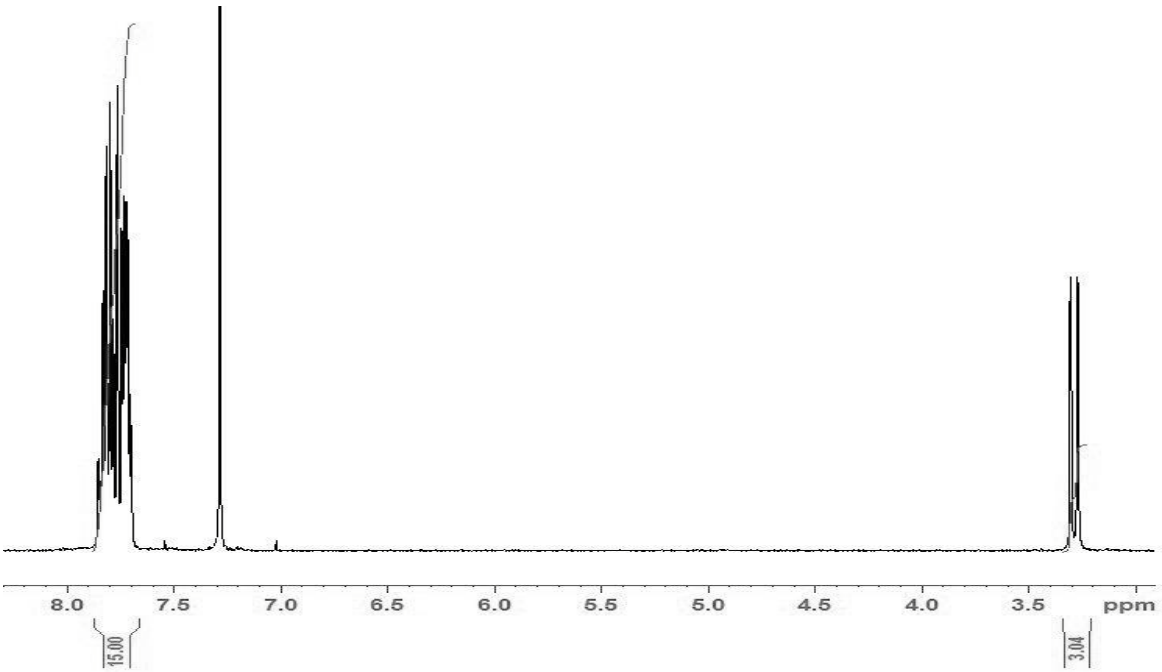

Methyltriphenylphosphonium iodide (18) (^{13}C (100.6 MHz, CDCl3):

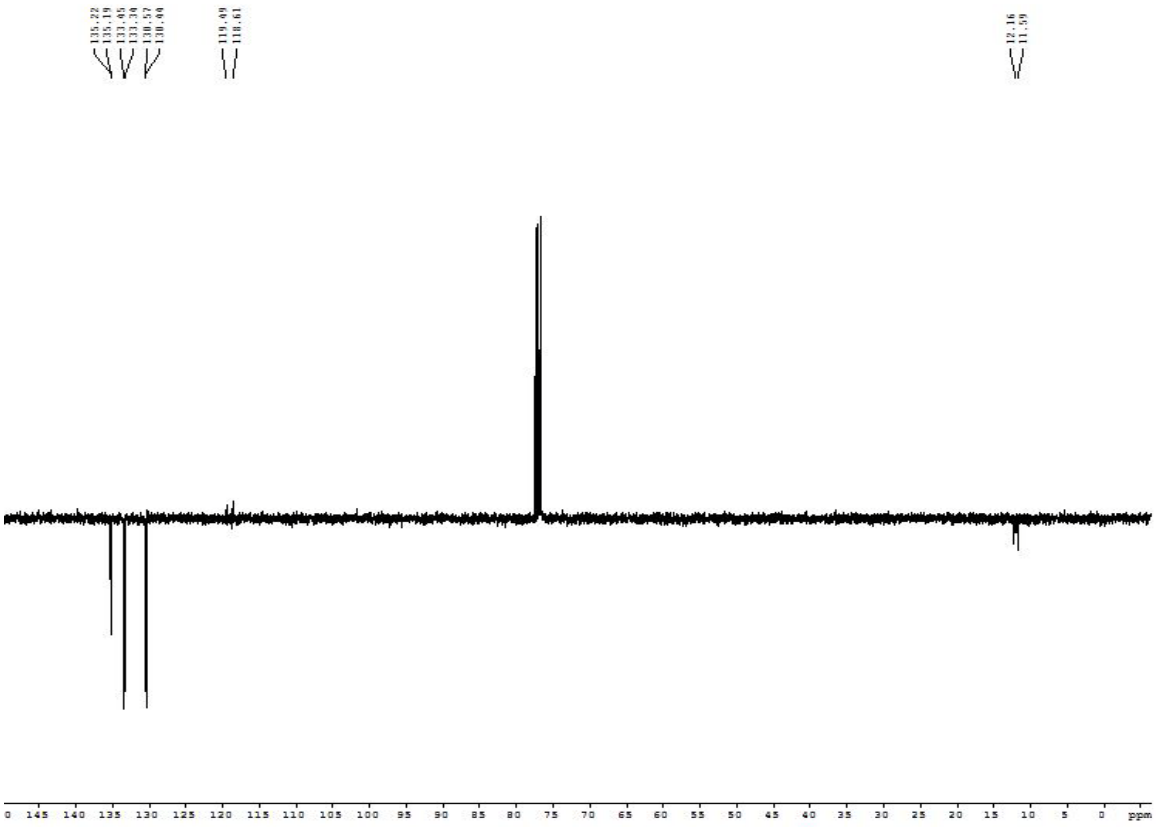

[D_3]-methyltriphenylphosphonium iodide (19) (^{1}H NMR (400.3 MHz, $CDCl_3$)